MAPPING THE RISK: VULNERABILITY ASSESSMENT OF COASTAL AQUIFERS TO TSUNAMI-INDUCED SALTWATER INTRUSION IN MAUI, HAWAII

A THESIS

Presented To

The Faculty of the Department of Environmental Science

The Colorado College

In Partial Fulfillment of the Requirements for the Degree

Bachelor of Arts

By

Sara A. Dixon

May 2022

Yong Wei

Dr. Yong Wei
Senior Research Scientist at the University of Washington

Charlotte Gabrielsen

Dr. Charlotte Gabrielsen
Assistant Professor of Environmental Science

TABLE OF CONTENTS

ABSTRACT

As the global mean sea level continues to rise due to climate change, tsunamis are projected to increase in intensity and frequency, which will disproportionately impact coastal communities globally. Numerous countries have been affected by long-term, negative impacts to their groundwater resources from tsunami-induced saltwater intrusion. Accordingly, it is important to develop effective methods for assessing risk of tsunami-induced saltwater intrusion in order to promote natural disaster preparedness and response strategies. This study evaluates how the integration of high-resolution probabilistic tsunami design-zone maps and risk assessment maps can be used to predict the extent and risk level of tsunami-induced saltwater intrusion in coastal aquifers on the Island of Maui in Hawaii, USA. I created tsunami design zone (TDZ) maps in ArcGIS Pro using a digital elevation model, the Probabilistic Tsunami Hazard Assessment (PTHA) method, and the non-hydrostatic NEOWAVE model. The resulting maps depicted flooding extent, flooding duration, and flooding depth. I also created a series of risk assessment maps based on several hypothesized drivers of saltwater-intrusion risk, including aquifer characteristics, topography, land cover, and well density data, to conduct a qualitative and quantitative risk analysis. Overall, I found that the census-designated places of Kahului and Kihei–Makena are extremely vulnerable to tsunami-induced saltwater intrusion. The combined use of probabilistic tsunami design zone maps and risk assessment maps, as described in this study, has the potential to serve as a useful tool to assist local governments and emergency and response management teams. As climate change continues to cause more severe tsunami-related impacts, Maui and other coastal regions around the world will become increasingly vulnerable to tsunami-induced saltwater intrusion, making the utilization of probabilistic tsunami design zone maps and risk assessment maps essential for long-term hazard preparedness and mitigation.

ACKNOWLEDGMENTS

I would like to thank Dr. Yong Wei for giving me the opportunity to be involved with his research and for encouraging me to expand this project in my thesis. Additionally, I would like to thank my thesis advisor, Dr. Charlotte Gabrielsen, for her help throughout the entire research and writing process. Thank you to Matt Cooney, the GIS Technical Director, for always being available and excited to provide guidance on my maps. I would also like to extend a thank you to my professor, Dr. Miro Kummel, for encouraging me throughout my time at Colorado College and during my thesis. Finally, I would like to thank my mom for her continued support throughout my life, especially during my four years at Colorado College. This thesis would not have been completed without everyone mentioned above and so many more.

INTRODUCTION

The climate is rapidly changing, and with change comes an increase in the intensity and frequency of natural disasters (Benevolenza & Derigne, 2018). The ocean covers 70% of the Earth's surface and is constantly interacting with the atmosphere. Global warming has provoked the melting of ice caps and glaciers and has increased the ocean's mean surface temperature (Mimura, 2013) by ~0.06°C per decade from 1901-2012 and ~0.095 per decade from 1979-2012 (Alexander et al., 2018). This has led to the largest increase in global mean sea level over the past 120 years; from 1901 to 1993, the global mean sea level was rising at a rate of 1.7 mm per year and since 1993, the rate has increased to 3.3 mm per year (Swapna et al., 2020). This unprecedented increase in global mean sea level is predicted to amplify both the frequency and severity of tsunami-induced flooding (Li et al., 2018).

Climate effects on tsunami frequency and intensity

Tsunamis are ocean waves caused by submarine earthquakes, underwater or coastal landslides, or volcanic eruptions (Gonzalez, 1999), and some are associated with meteorological events more frequently than previously known (Angove et al., 2021). Most earthquake-generated tsunamis occur in the subduction zones around the Pacific Ocean Basin, also known as the "Ring of Fire," an area comprised of many moving and colliding tectonic plates. The moving of tectonic plates causes earthquakes and volcanic eruptions, which in turn, can generate tsunamis (Hulick, 2016). Coastal communities and islands that are positioned around the Ring of Fire are and will continue to be threatened by tsunamis and sea-level rise independently, but also in combination, given the projected increase in tsunami intensity and frequency caused by sea-level rise (Bernard & Titov, 2015).

While small earthquakes generally pose little to no threat to major tsunamis, even modest rises in sea level are projected to increase tsunami inundation distances and depths on land (Dura et al., 2021; Li et al., 2018). These climatic changes will also affect wave generation and propagation, resulting in faster and more intense waves near the shore (Yavuz et al., 2020).

Tsunami inundation models for natural disaster preparedness

Within the past 20 years, two of the deadliest and most expensive tsunamis have occurred. In December 2004, a tsunami was triggered by a magnitude 9.3 earthquake that occurred off the coast of Sumatra and hit 18 countries surrounding the Indian Ocean (Illangasekare et al., 2006). More than 200,000 people were killed by this devastating tsunami that reached numerous coastlines globally (Titov et al., 2005). In March 2011, another tsunami was triggered by a magnitude 9.0 earthquake near Japan, causing more than 20,000 causalities, and impacting over 25 countries in the Pacific Rim (Kaihotsu et al., 2017). The tsunami-load-induced damages to coastal infrastructure and communities were substantial: more than 250,000 buildings along Japan's coastline collapsed predominantly due to the tsunami (Chock et al., 2013). These large-scale impacts led to the development of the first design standard of tsunami loads and effects on buildings and structures within the tsunami inundation zone (ASCE, 2017).

In response to the projected increase in tsunami frequency and intensity, several researchers have begun to develop technologies that can help communities better prepare for tsunamis and similar natural disasters (Merati et al., 2009; Sepúlveda et al., 2021). While it remains difficult to predict when and where a tsunami will occur, tsunami warning centers have been working to improve the warning systems and technologies that track the earthquakes that generate a tsunami (Bernard & Titov, 2015). Furthermore, tsunami warning centers have

developed models, known as the short-term inundation forecasting for tsunamis (SIFT) system (Titov, 2009), that are capable of predicting tsunami extents, which in turn enables communities to better prepare themselves and their infrastructure for future tsunamis (Tang et al., 2009 and 2012; Titov, 2009; Wei et al., 2008 and 2013).

Forecast models can provide estimates of wave arrival time, height, current speed, and inundation areas with a lead time of minutes to hours before the tsunami arrives (Bernard & Titov, 2015; Merati et al., 2009). Inundation models, on the other hand, are often used to assess long-term tsunami impacts on coastal communities resulting from deterministically- or probabilistically-determined tsunami scenarios, in the context of projected sea-level rise. Inundation models output maximum water elevation, inundation depth, current speed, and inundation extent, all of which can be displayed as maps. These models can provide communities with a realistic idea of probable tsunami flooding extents to help them better prepare for the effects of future tsunamis (Robertson, 2020b).

Tsunami-induced saltwater intrusion

Flooding events from tsunamis may result in saltwater infiltration into aquifers, which can detrimentally impact those who rely on groundwater for drinking and other basic needs (Liu & Tokunaga, 2019). Saltwater intrusion into coastal aquifers is an issue that many communities have already been experiencing as a result of climatic and land-use changes, as well as the over-pumping of aquifers. These factors can lead to several negative impacts including reduced aquifer recharge, decreased groundwater levels, and saltwater intrusion (Jasechko et al., 2020). Tsunami-induced saltwater intrusion, while not as widely studied as other mechanisms by which saltwater intrusion occurs, may be especially detrimental.

Given that major freshwater losses may occur if communities are not prepared for increased saltwater intrusion or large-scale flooding events, it is imperative that scientists continue to study the processes by which saltwater intrusion occurs. Based on studies of past occurrences, researchers have identified four main mechanisms driving tsunami-induced saltwater intrusion: (1) rapid infiltration of saltwater through the ground surface during the inundation period; (2) ponding of saline water on the ground's surface that leads to percolation and the mixing of fresh and saltwater; (3) direct infiltration of saltwater into wells; and (4) lateral intrusion of saltwater that disturbs the saltwater-freshwater interface (Kumaraguru et al., 2007; Liu & Tokunaga, 2019; Villholth, 2007).

Geographic Information Systems (GIS) have provided a useful tool for predicting saltwater intrusion risk in coastal communities, as it enables the identification and prioritization of locations that will be impacted based on natural and anthropogenic features. If maps can be developed with sufficiently high spatial resolution, individual households and businesses could be informed if they are at a high risk of saltwater intrusion (Kennedy, 2012). Risk assessment maps can take into account numerous characteristics that may influence how vulnerable a region is to saltwater intrusion (Kennedy, 2012; Klassen & Allen, 2017), and in turn, characterize the impact that these characteristics may have on groundwater salinization owing to more intense tsunamis.

Drivers of saltwater intrusion risk

Following the tsunamis in Sumatra and Japan described above, numerous coastal areas worldwide experienced saltwater intrusion into groundwater aquifers; however, intrusion

severity varied based on several factors, including aquifer type, topography, land cover (Delhi, 2017), and the location of wells (Illangasekare et al., 2006).

Aquifers vary widely depending on how they were formed, underlying bedrock characteristics, if they are in contact with seawater, and whether they are confined (below the land surface and saturated with water) or unconfined (open to the surface, recharged by water infiltrating directly through the overlying soil). In combination, these various attributes influence the speed that water travels throughout an aquifer and in turn, how fast it recharges (Kennedy, 2012).

Aquifers consist of many types of bedrock, but the two most relevant to this study are sedimentary and perched. Sedimentary aquifers have a low permeability which impedes the lateral movement of groundwater and discharge into the ocean. This impacts an aquifer's ability to recover naturally after groundwater salinization (Scot Izuka et al., 2015). Perched aquifers sit on an impermeable layer of sediment which can limit the amount of infiltration, storage, and recharge, putting the aquifer at higher risk for intrusion (Yousif & Bubenzer, n.d.).

The differences in permeability between confined and unconfined aquifers are another determinant of how vulnerable an area may be to saltwater intrusion. Confined aquifers have an impermeable layer of the deposit that isolates them from contamination on the surface, but it also inhibits natural recharge from surface waters. Due to the slow recharge rates, confined aquifers also have a low storage capacity making it easier to pollute and harder to reverse contamination that may occur. Unconfined aquifers, on the other hand, lack an impermeable layer, so they are connected to the Earth's surface, allowing for direct infiltration through the ground. While this may enhance their risk of pollution, they can typically recover naturally at a faster rate as surface water infiltrates and flushes out the contaminants (Şen, 2015). In some areas, desalinization and

decontamination efforts have been used to return groundwater chemistry to pre-tsunami conditions (Delhi, 2017; Kaihotsu et al., 2017), whereas other regions have relied on natural groundwater decontamination and desalination by letting precipitation infiltrate and washout pollutants and saltwater (Kaihotsu et al., 2017).

Other characteristics that can strongly influence how susceptible an area is to saltwater intrusion include topography, land cover, and well density. For example, low-elevation (Delhi, 2017) and urbanized (White & Kaplan, 2017) areas are more likely to be impacted by extensive tsunami flooding and saltwater intrusion than areas with more variable elevation (Delhi, 2017; Klassen & Allen, 2017) and forests (Carlos et al., 2011; Delhi, 2017). Furthermore, depressions in the ground's surface that are filled with salt water for prolonged periods of time are known to cause delayed spikes in aquifer salinity levels, thus increasing an area's risk for saltwater intrusion (Violette et al., 2009). Infrastructure and impervious surfaces can reduce saltwater intrusion directly through the ground, potentially decreasing the prevalence and rate of salinization. Alternatively, impervious surfaces may reduce natural aquifer recharge as water is unable to penetrate through them.

In coastal areas vulnerable to saltwater intrusion, where high densities of coastal drinking wells also exist, impacts to aquifers may be further exacerbated. Following extreme tsunami flooding, aquifers may be contaminated with salt water and chemicals directly through the ground's surface and open wells (Illangasekare et al., 2006; Inui et al., 2012; Violette et al., 2009; Bhattachan et al., 2018).

While the National Oceanic and Atmospheric Administration (NOAA) has determined that the duration of coastal flooding is being intensified by rising sea levels, knowledge regarding its effects on saltwater intrusion risk remains limited (Pezza & White, 2021).

Researchers studying the effects of the 2004 tsunami in Sri Lanka found that flooding of short durations and high volumes of water led to infiltration through the surface due to high ground permeability (Villholth & International Irrigation Management Institute., 2005). Long flooding durations can lead to equally detrimental effects as water volume though because standing water has more time to infiltrate into the aquifer (Violette et al., 2009).

Tsunami vulnerability in Hawaii

Hawaii – a state in the United States located in the Pacific Ocean about 2,000 miles west of the continental U.S. – is one region particularly vulnerable to the effects of tsunamis, owing to its position at the center of the Ring of Fire, small size, low-lying coastal areas, and large population densities near its shores (State of Hawai‘i - Hazard Mitigation Plan, 2018). Since 1812, Hawaii has experienced over 100 tsunamis of varying severity. Although there has not been a tsunami in Hawaii as destructive as the tsunami that occurred in 1946 (Macdonald et al., 1946), Maui's government recognizes that climate change will continue to increase the intensity and frequency of natural disasters. In 2019, the Islands of Maui and Hawai'i declared climate emergencies, and a state-wide climate emergency was announced two years later in 2021 (USA: First American State Declares a Climate Emergency - Climate Emergency Declaration, 2021).

In July 2021 and February 2022, the Island of Maui experienced groundwater shortages resulting from extreme periods of drought. The droughts in Hawaii were caused by unseasonably low levels of precipitation and higher than average surface temperatures (Cerizo, n.d., 2022). Droughts increase an aquifers' risk for saltwater intrusion since lower water tables can enable saltwater to intrude upwards or horizontally and lower rates of precipitation lead to less groundwater recharge through the Earth's surface (Gingerich et al., n.d.). Droughts coupled with

the increase in intensity and frequency of tsunamis due to sea-level rise will amplify Hawaii's risk of tsunami-induced saltwater intrusion (Firing & Merrifield, 2004). As tsunamis become more powerful and frequent, there will be an increase in the volume of water on land and the mechanisms for saltwater intrusion (*e.g.* direct infiltration through the surface, ponding of water, flooding into wells, and changes in the saltwater-freshwater interface (Liu & Tokunaga, 2019).

Although Hawaii has not experienced large-scale impacts from tsunami-induced saltwater intrusion in the past, climate change is predicted to exacerbate the detrimental effects of tsunamis on Hawaii's environment and natural resources (Gingerich et al., n.d.). Within the last decade, Hawaii has sought to improve its technology and advance research to mitigate the effects of future tsunamis on people, the environment, and infrastructure. Hawaii's Department of Defense released a report in 2018 that provided a quantitative risk assessment of environmental, economic, infrastructural, and humanitarian losses based on the Great Aleutian Tsunami inundation area (*State of Hawai'i - Hazard Mitigation Plan*, 2018).

In areas of the United States that are considered high-risk for tsunamis, such as Hawaii, tsunami design zone (TDZ) maps have been developed to visualize worst-case scenario tsunami characteristics such as flooding extent, run-up elevation, inundation depth. In Hawaii, these high-resolution (every ~10-m in horizontal spaces) TDZ maps are based on a Probabilistic Tsunami Hazard Analysis (PTHA) method (Thio et al., 2010; Wei et al., 2015; Chock et al., 2018), and computed using a tsunami inundation model – known as the non-hydrostatic NEOWAVE model (Yoshiki et al., 2011). TDZ maps were created for the Island of Oahu with the aim of being compatible with the American Society for Civil Engineers (ASCE) 7-22 Minimum Design Loads and Associated Criteria for Buildings and Other Structures guidelines (ASCE, 2022) maps for other islands are expected to be integrated into the ASCE 7-28 version by 2028. In combination,

the ASCE guidelines and TDZ maps aid engineers in determining the standard for new buildings to be built or reinforced to withstand tsunami flooding, particularly buildings of high importance (*e.g.*, hospitals, fire departments, and economic centers) (Robertson, 2020a).

While the effects of tsunamis in Hawaii are widely acknowledged and studied, limited research exists regarding the potential impacts of tsunami-induced saltwater intrusion. Accordingly, it is important to understand the factors and risk levels of the aquifers in terms of saltwater intrusion caused by extreme tsunami hazards. To my knowledge, these risks have not been studied utilizing modeling datasets offering high-resolution spatial distributions of inundation depth, flow velocity, and impacting duration.

Objective

This study evaluates how the integration of high-resolution probabilistic tsunami design zone and risk assessment maps can be used to predict the extent and risk level of tsunami-induced seawater infiltration in coastal aquifers on the Island of Maui in Hawaii, USA. Drawing upon previous research on tsunami-induced saltwater intrusion, this study considers the relative risk of tsunami-induced saltwater intrusion as it relates to the spatial distribution of several hypothesized drivers including aquifer characteristics, topography, land cover, well density, flooding duration, flooding extent, and flooding depth. By using GIS to map the relative risk levels of coastal aquifers in the context of extreme flooding events, this study seeks to provide a tool to assist local governments and emergency and response management teams in long-term hazard mitigation planning.

METHODS

Study site

This study was conducted in Maui, Hawaii, USA within the census-designated places of Kahului and Kihei - Makena (Fig. 1). These two regions on Maui have the highest population densities and are low-lying, making them particularly vulnerable to tsunami impacts. Overall, Maui has a tropical climate that can be characterized by its mild temperatures, moderate humidity, and northeasterly trade winds. The warmest months in Maui occur between May and October, and "winter" occurs between October and April. At sea level, the average daytime temperature in the summer is 29.4 °C and the average daytime winter temperature is 25.6 °C (*Climate of Hawai`i*, n.d.). Maui's volcanoes influence the flow of air and precipitation across the island through the orographic effect. The mountains make the air moist, and warm on the windward side which then precipitates and leaves the air dry and cool on the leeward side. The Tradewinds and elevational differences cause variations in precipitation across Maui, so it is common for locations at higher elevations to receive more rain than the lowland areas (*Climate of Hawai`i*, n.d.). The high-altitude areas of Maui see annual rainfall as high as 10 meters, whereas the low-lying areas have an annual rainfall of 0.2 – 0.7 meters (Giambelluca et al., n.d.).

Maui is the second-largest island in Hawaii and is comprised of two large shield volcanoes connected by a lowland isthmus formed by sedimentary deposits. The West Maui volcano has an elevation of 6,788 ft and the East Maui volcano has an elevation of 10,023 ft (Mink & Lau, 1992). Volcanic aquifers – also known as dike or basalt aquifers – currently make up most of the island and were formed when the island was created. These aquifers are considered among the most productive given their high permeability. In addition to the volcanic aquifers that dominate Maui, some sedimentary aquifers were also formed as a result of the

isthmus that developed between the East and West Maui volcanoes (Scot Izuka et al., n.d.). These sedimentary aquifers have lower permeability which limits groundwater flow between aquifers and discharge to the ocean (Adebayo & Abraham, 2018). Eastern Maui consists of perched aquifers which are characterized by water sitting on an impermeable layer of fine volcanic ash or clay soil. Flank aquifers are also present in Maui and are generally larger horizontally and carry basal water (*i.e.*, groundwater floats on top of a body of salt water). Lastly, dike aquifers form when magma stops flowing and cools. This creates sheets of nonporous rock that trap freshwater vertically.

Probabilistic Tsunami Design Zone (TDZ) maps

ASCE recently updated its 7-22 Minimum Design Loads and Associated Criteria for Buildings and Other Structures guidelines for 2022. To create a product compatible with the new ASCE 7-22 guidelines for Kahului and Kihei–Makena, I created high-resolution probabilistic Tsunami Design Zone (TDZ) maps from a combination of (1) a digital elevation model; (2) the method of Probabilistic Tsunami Hazard Assessment (PTHA); and (3) the non-hydrostatic NEOWAVE model (Robertson, 2020a). All spatial data were projected to the same coordinate system, WGS 1984 UTM Zone 4N, and the resulting TDZ maps had a spatial resolution of ~10-meters.

The digital elevation models (DEMs) used in the Hawaii mapping study were compiled using the most comprehensive bathymetry and topography for the Pacific Basin from open and semi-open sources. The topography was derived from 10 and 30-m USGS DEMs, which include the SRTM (Shuttle Radar Topography Mission) data, with the LiDAR topography at 1-m horizontal resolution extending from the shoreline to the 15 m (50 ft) elevation contour. Per

ASCE's requirement, the topography is processed to "bare earth" with vegetation and buildings removed. The primary nearshore bathymetry source is the SHOALS (Scanning Hydrographic Operational Airborne LiDAR Survey) dataset that extends from the shoreline to approximately 40-m water depth at 4-m horizontal resolution. Data from hydrographic surveys and nautical charts supplement the near-shore bathymetry, mostly inside harbors and marinas. These DEMs were integrated to obtain model grids at a 10-m spatial resolution with all water depths and land elevations relative to the Mean Higher High Water - the mean of the highest tide recorded each day over the National Tidal Datum Epoch (usually a total of 19 years).

The PTHA model was used as an input for the creation of the TDZ maps to assess the 2,500-year, 2% probability in 50 years of tsunami risks based on thousands of tsunami scenarios. The model takes into account epistemic uncertainties, due to an incomplete understanding of the natural process (e.g. earthquake fault segmentation, slip rate, and recurrence model), and aleatory, due to the random nature of a process (such as modeling uncertainty, earthquake dip and slip). The model estimates the 2,500-year inundation depth, runup elevation, or momentum flux at given locations within hours after the tsunami waves arrive and inundate, and the results are then used to determine which locations are considered high risk for tsunamis. From the PTHA model, Kahului and Kihei–Makena were identified as high-risk and therefore served as the two locations that I focused on for this study.

The final input – the computational results from the non-hydrostatic NEOWAVE model – is commonly used to inform the ASCE guidelines (Robertson, 2020a). For the regions of Kahului and Kihei–Makena, the NEOWAVE model results were based on a 9.49 magnitude Aleutian-Trench and a 9.53 magnitude Kamchatka-Trench earthquake scenario (Yamazaki et al., 2011). I used the following data in this study: inundation area indicated by run-up elevation points (to

visualize the maximum onshore flooding area as a polygon), maximum inundation depth (to demonstrate the local flow depth present on land as a raster), and flow duration (the number of seconds the water was present on land at various thresholds of the inundation depth as polygons) (Fig. A5).

I created all probabilistic TDZ maps using ArcGIS Pro version 2.8.6 (ESRI). To do so, I used the maximum tsunami run-up data in conjunction with digital elevation models to create the flooding polygons for Kahului and Kihei–Makena. I used polygons, rather than just the run-up line, to visualize clearer tsunami flooding zone boundaries and allow for easier and more consistent data comparisons between the maps. The first set of data inputs that I used to create the run-up line for the two locations were XYZ files, where X represented the longitude, Y represented the latitude, and Z was a height value, if it applied. In the run-up data, Z values were not derived since each longitude and latitude values map the points that create the run-up line. I created the run-up line using the "Point to Line" geoprocessing tool in ArcGIS Pro, which creates a continuous line from points. The XYZ values were coded in MATLAB to ensure that the points were ordered correctly and that the line would be continuous between consecutive points. Once the line was created, I used a digital elevation model to derive the 20-m bathymetric contour line, instead of directly using the shoreline (0-m contour), which was then connected to the run-up line with the "Extend" tool. The polygon created in this way appears to be more compatible with ASCE map products that require no "wet" points inside the inundated area. To turn the run-up and contour lines into one continuous polygon, I used the "Merge" geoprocessing tool. Finally, I used the "Feature to Polygon" tool to convert the polygon into a shapefile that could be more easily edited in downstream analyses.

The second data set, the inundation depth, was also in XYZ file format, with the Z values representative of the maximum inundation depths at various latitudes (Y) and longitudes (X) for every location (or grid point) wetted by the tsunami. I used flow depth to understand how different water depths on land, during and after tsunamis, can impact an area's risk of saltwater intrusion. I uploaded the flow depth data into ArcGIS Pro and converted it into a shapefile using the "Feature Class to Shapefile" geoprocessing tool. I then converted the points into a raster with the "Point to Raster" geoprocessing tool and used the stretch symbology to create a color scale that displayed unique colors for the flow depths from 0 to 9 meters.

The third and final data set – flow duration – was used to understand the impacts water duration on land can have on a region's susceptibility to saltwater intrusion after a tsunami. Flow duration data was also in XYZ file format, where the Z values corresponded to the amount of time in seconds that the water was at or above a specified depth threshold. Five different depth thresholds were analyzed, ranging from 1-m to 5-m. Similar to the XYZ input data described above, the flow duration data points were uploaded as XYZ data and converted into a shapefile with the "Feature Class to Shapefile" geoprocessing tool, followed by conversion into a raster using the "Point to Raster" geoprocessing tool.

Development of tsunami-induced saltwater intrusion risk assessment maps

I created a series of risk assessment maps to illustrate the relative influence of several different anthropogenic and natural landscape features known to affect an aquifer's vulnerability to tsunami-induced saltwater intrusion. Specifically, I characterized: (1) well density, (2) combined slope and distance from shore, (3) aquifer types, and (4) land cover. I then overlayed

the tsunami design zone maps onto these maps to make inferences regarding the susceptibility of different locations within the study area to tsunami-induced saltwater intrusion.

To calculate the density of wells in Maui, I used spatial data from the Hawaii State Water Wells project through the Hawaii Groundwater & Geothermal Resources Center. Digitized well location data spanned from 1987 through 2012. More recent data was unavailable, as spatial data on well locations submitted to the Commission of Water Resources Management office in Hawai'i has not yet been digitized (Hawai 'i Groundwater & Geothermal Resources Center, (n.d.).

The Hawai'i State Water Wells project data consists of the well names and corresponding global positioning system (GPS) coordinates (Fig. A1). I used the "Point Density" geoprocessing tool and symbology tool to create five different groupings of equal densities. I assigned each grouping a rating of one to five to symbolize a low to high risk of saltwater intrusion based on well density (Fig. 6). In this study, the five well density groupings ranged from three wells to 16 wells (Table A1).

To derive topographic slope, an important variable that may determine flooding and saltwater intrusion extents, I used the 2019 light detection and ranging (LiDAR) data from the Hawaii Statewide GIS Program. The LiDAR dataset was purchased by the County of Maui from Vexcel, Inc and was collected at a spatial resolution of 1-m. Although LiDAR data were not collected for the entire island of Maui, both study sites (Kahului and Kihei–Makena) had full LiDAR coverage (Vexcel Inc., 2019). To derive slope, I imported the LiDAR data into ArcGIS Pro and used the "Slope" geoprocessing tool to derive slope from the elevation data (Fig. A4). In the symbology settings, I classified slope into five equal interval classes ranging from 0–90 degrees (Table A1).

To create the distance from shore buffer map, I used a cartographic boundary shapefile for Hawaii (U.S. Bureau of the Census, 2020) and ArcGIS Pro to create five different distance bands within the shapefile for Maui. This is important because varying distances from shore will impact the susceptibility of an area to flooding and saltwater intrusion during a tsunami. I created the distance from shore map using the "Multiple Ring Buffer" geoprocessing tool in ArcGIS Pro, which creates buffers at specified distances around or within an input feature. I created variable distance buffers by using the island of Maui shapefile and inputting the following distances from shore, in meters: 0, 500, 1000, 1500, and 2500 (Table A1; Fig. A4).

Since both slope and distance from shore in combination determine saltwater-intrusion risk (*e.g.*, a location of shallow slope that is also close to the shore would have a much higher risk compared to an area with steep slope located further from the shore), I used ArcGIS Pro to combine the slope and distance from shore maps. To do so, I first converted both shapefiles to rasters and resampled pixels to a 1-m spatial resolution. Each pixel on the two maps had a risk value assigned to it, ranging from 1 to 5, with 1 representing the lowest risk and 5 representing the highest risk level. I then used the "Raster Calculator" geoprocessing tool to calculate the average risk across both the slope and distance from shore maps. Because slope is predicted to contribute more to determining relative risk than distance from shore (*e.g.,* a shallow slope within a flooding area would put an area at higher risk of saltwater intrusion no matter the distance from shore), I weighted the slope layer by multiplying the risk values by a factor of three. Next, I summed the new slope and distance to shore rasters and divided the result by two to average the values of each cell across the two rasters. The calculation used was ((Slope*3) + (Distance))/2.

Once I created a combined slope and distance from shore raster layer, I again used the "Raster Calculator" to combine the well density layer with the combined slope and distance layer. Because the attribute tables for the well density and combined slope and distance layers were on the same scale of one to five, I summed the cell values of the two maps and averaged them using the calculation ((Dist/Slope + Well Density)/2)). This created a new scale that ranged from 2–10, since the minimum risk value on both maps was one and the maximum was five. This exacerbated the high well density areas that were the closest to the shores and put a smaller emphasis on areas that were further from the shore and outside of the flooding zones in Kahului and Kihei–Makena.

The aquifer data used in this study were created and delineated by the Hawai'i State Department of Health (DOH) in 2014 and were last updated in 2022. This study used the aquifer data to show how different aquifer characteristics can influence saltwater intrusion susceptibility. The aquifer variables included: whether the aquifer was in contact with seawater or not; the bedrock type; and whether the aquifer was confined or unconfined (Fig. A2). The DOH aquifer dataset provides a feature layer with polygons with attributes related to each of variables described above (State of Hawaii GIS Program, n.d.). I uploaded the DOH aquifer dataset to ArcGIS Pro as a feature layer, used the symbology tool to change the colors for the aquifer types to make the classes easier to visualize, and created a new attribute table to make the aquifer characteristics easier to differentiate.

Finally, I used the 2011 National Land Cover Data (NLCD) data set to illustrate how different land cover types in Maui can lead to enhanced saltwater intrusion and damage to natural and built environments. The NLCD product presents, at 30-m spatial resolution, a land cover assessment of Hawaii. It was developed from a combination of satellite data and ancillary

data sources (Homer et al., 2015). To create a more simplified land cover dataset relevant to the objectives of this study, I reclassified the NLCD dataset into 10 land classes (from an original dataset of 17 classes) using ArcGIS Pro. I then used the" Extract by Mask" geoprocessing tool to clip the land cover layer to each of the flooding polygons (Fig. A3).

After creating each of the separate risk assessment maps, I overlayed the resulting flooding polygons (Fig. 2) to visualize risk and susceptibility to saltwater intrusion as it related to anthropogenic and natural features within each of the probabilistic flooding extents.

Relative risk assessment by land cover and aquifer types

To analyze the percentage of land cover and aquifer types present within each of the five risk categories, as defined in the combined slope and distance from shore map, I used the "Tabulate Area" geoprocessing tool in ArcGIS Pro. I chose to use the combined slope and distance from shore map to determine risk categories because understanding how varying slopes and distances from shore in conjunction with land cover and aquifer types allowed for a deeper analysis of the risk for tsunami-induced saltwater intrusion in Kahului and Kihei–Makena. For example, a particular land cover type within a high-risk zone may be a low threat while a different land cover type within a high-risk zone may lead to enhanced saltwater intrusion. To prepare the data to input into the "Tabulate Area" tool, I clipped both layers to the extents of the flooding polygons and reclassified them on a scale from one to five. The tool then calculated the percentage of each land cover or aquifer type that overlapped with the five separate risk levels on the slope and distance from shore map. I then exported the tabulated data into Excel and calculated the percentages for the proportion of each aquifer or land cover type that fell within each of the five risk categories. This is important to understand because certain land cover and

aquifer characteristics increase the chance of saltwater intrusion, so higher percentages of vulnerable factors in the "Risk 5" category, for example, may lead to a heightened risk of saltwater intrusion.

RESULTS

Probabilistic TDZ maps

The flooding polygons that I developed for the areas of Kahului and Kihei–Makena showed that the maximum probabilistic flooding extent mainly impacts the two most densely populated regions of Maui. The TDZ maps completed for two communities in Maui – Kahului and Kihei–Makena – indicate extensive tsunami inundation impact that can reach most of the aquifers in these two areas. Additionally, the probabilistic flooding extents are expected to reach farther onto land in areas with high amounts of built infrastructure such as roads and buildings (Fig. 2).

The maximum flow depth maps generally had the highest values in areas closest to the shore and the lowest values farthest from the shore. In Kahului, the depth ranged from zero meters to 20 meters (Fig. 3a) and in Kihei–Makena the depth ranged from zero meters to 13.5 meters (Fig. 3b). In both maps, there were some smaller areas further from the shore where the maximum flow depth was higher than the surrounding regions.

The flow duration maps had a range of 60 seconds to over 25,000 seconds, which is equivalent to seven hours. There were similar overall patterns in Kahului (Fig. 4) and Kihei–Makena (Fig. 5), where the 5-m water depth threshold had a wider range of flow durations, while the lower flooding depths had lower flow durations. In Kahului and Kihei–Makena, the 2-m and 3-m flow duration maps depicted distinct areas where the flow duration was significantly longer

than the surrounding zones. There were also several small areas far from the shore that exhibited long flow duration, even when the water depth threshold was only 2-m and 3-m.

Spatial assessment of tsunami-induced saltwater intrusion risk by driver

I found that Maui had the highest densities of wells in the regions with higher populations while the rest of the island had low well densities. Of the two study sites, Kahului had a larger density of wells than the region of Kihei–Makena (Fig. 6). Within the study sites, the highest risk of saltwater intrusion based on well density alone was found near the shore in Kahului and in the area that is expected to experience the farthest tsunami run-up. In Kihei–Makena, I found that the risk of saltwater intrusion through wells was low, even close to the shore. In both study sites, there were large areas located along the shore with little to no risk of saltwater intrusion (Fig. 6).

I found that the areas with the highest risk of saltwater intrusion based on slope and distance from shore existed near the coast in Kahului and Kihei–Makena. Not all areas on Maui follow this trend, as there were some areas close to the shore where the risk of saltwater intrusion was low (*e.g.* on the northeastern side of Maui; Fig. 7). Despite this varying degree of risk, the overall trend across both study sites suggests that the closer an area is to the shore, the more susceptible it is to tsunami-induced saltwater intrusion (Fig. 7).

By combining the well density layer with the slope and distance from shore layer, I created a map that assessed the overall risk of saltwater intrusion for the Kahului and Kihei–Makena regions. Most of the combined risk assessment map showed a low risk of tsunami-induced saltwater intrusion, with a few exceptions near the shore of Kahului and Kihei–Makena. Kihei–Makena has a medium-level risk of saltwater intrusion along the shore while Kahului has the highest and largest risk of saltwater intrusion within the probabilistic flooding zone (Fig. 8).

Distribution of aquifer and land cover types by risk class

I calculated the proportions of each aquifer and land cover type within the five risk categories from the combined slope and distance from shore map to aid in determining how vulnerable an area is based on the susceptibility of the aquifer or land cover type in combination with the already present risk as defined by the combined slope and distance from shore map (Fig. 7).

Although Maui has numerous aquifers of varied types owing to its unique geologic past, only two different classified aquifer types existed within the flooding zones. After overlaying the aquifer map (Fig. A2) with the slope and distance from shore map in Kahului (Fig. 9), I found that of the sedimentary aquifers that are unconfined and in contact with seawater aquifer, 70% fell within the Risk 5 category and 25% fell within the Risk 4 category. Of the perched aquifers that are unconfined and not in contact with seawater, 33% fell within the Risk 5 category, and 61% fell within the Risk 4 category (Table 1). Additionally, I found that perched aquifers were present across 23% of the flooding zone, while sedimentary aquifers were present across 77% of the flooding zone (Table 1).

In Kihei–Makena (Fig. 10), I found that 82% of the sedimentary aquifer fell within the Risk 5 category while 63% of the perched aquifer fell within the Risk 5 category and 24% fell within the Risk 4 category (Table 1). Sedimentary aquifer types were within 95% of the Kihei–Makena flooding zone and perched aquifers were within 5% of the flooding zone (Table 1).

In Kahului (Fig. 11), I found that the land cover combined with the slope and distance from shore map showed that the classes with the highest percentages in the Risk 5 category were (in order from highest to lowest): open water, impervious surfaces, wetlands, and developed open spaces (Figure 11a). Of all the open water within the study area, 83% fell within the Risk 5

category. For impervious surfaces, 77% fell within the highest risk category. Wetlands and open spaces developed have around 71% that fell within the same category (Table 2). Impervious spaces comprised the largest proportion of land cover type within the Kahului flooding zone at 31% and open water consisted of 18%. Wetlands and developed open spaces made up 4% and 13% of the study sites, respectively (Table 2).

For Kihei–Makena, the flooding zone was more concentrated near the shore, so nearly all the land cover types had a large percentage contained within the Risk 5 ranking (Fig. 12). For every land cover class, 70% or more fell within the flooding zones, so considering the proportion of each land cover type present was integral (Table 2). Open water and impervious spaces comprised the highest percentage of land cover present with almost 30% each, while open space developed, and evergreen comprised the next highest percentages at 13% (Table 2).

DISCUSSION

In this study, I assessed the utility of integrating high-resolution probabilistic tsunami design zone and risk assessment maps to predict the extent and risk level of tsunami-induced saltwater infiltration in coastal aquifers on the Island of Maui. To do so, I identified and visualized the spatial distribution of seven factors identified by previous studies and historical accounts as important determinants of saltwater intrusion risk (Delhi, 2017; Illangasekare et al., 2006; Kennedy, 2012; Pezza & White, 2021; Şen, 2015; Violette et al., 2009; White & Kaplan, 2017; Yousif & Bubenzer, n.d.): flooding extent, flooding depth, flooding duration, well density, topography, aquifer characteristics, and land cover. The resulting risk maps are anticipated to be useful to local governments and emergency and response management teams in their long-term hazard mitigation planning. Furthermore, given their relatively high spatial resolution, these map

products provide individual homes and businesses the ability to assess their probabilistic risk of tsunami-induced saltwater intrusion.

Implications of inundation depth and duration on saltwater intrusion risk

The probabilistic TDZ maps provide a realistic and useful flooding scenario that enables a prediction of the effects that a tsunami could have on a given region. These maps, used in conjunction with risk assessment maps, can provide a better understanding of the factors that influence how vulnerable coastal communities are to tsunami-induced saltwater intrusion. Based on both the maps created and the knowledge gained from researching previous tsunami events, it is important to consider several factors in combination, including the tsunami run-up elevation, inundation depth, inundation duration, well density, topography, aquifer characteristics, and land cover.

Overall, the probabilistic inundation depth and duration maps showed that areas close to the shore in Kahului and Kihei–Makena are expected to experience high inundation depths and distances due to their proximity to the ocean during tsunami events. This puts these locations at particularly high risk for saltwater intrusion since the volume and duration of water near the shore allows more time for saltwater to infiltrate through the ground surface or through wells (Pezza & White, 2021; Violette et al., 2009). Although most areas in Kahului and Kihei–Makena follow trends of high to low inundation values with increasing distance from the shore inland, I observed some areas located farther from the shore with abnormally high depth and duration values in relation to their surrounding areas. These locations were identified as a result of the NEOWAVE model's inclusion of topographic features when creating probabilistic TDZ maps (Robertson, 2020a). This resulted in high positive correlations between depressions in the ground

and high inundation depths and durations. Following tsunami events, depressions in the ground can cause water to pool for long periods of time, making it harder for saltwater to retreat or infiltrate quickly. In Kahului and Kihei–Makena, many areas near the shore and some areas with depressions had water durations that exceeded 7 hours at the 3-m, 2-m, and 1-m thresholds. After the 2004 tsunami, scientists in Sri Lanka found that depressions in the ground caused delayed spikes in groundwater salinity levels since the pools of water had more time to infiltrate into the aquifers (Villholth, 2007). Since pools of water cause heightened levels of saltwater intrusion, it is important for Kahului and Kihei–Makena to be aware of the areas with high inundation depths and durations.

Utility of risk assessment maps for disaster preparedness

Based on the well density map, I found that Kahului has a high risk for saltwater intrusion and Kihei–Makena has a mild- to moderate risk, which may be explained in part by Kahului's larger population size. Wells in Kahului are concentrated near the harbor, where most buildings are also located, whereas the wells in Kihei–Makena are evenly distributed along the shore. Many of the large-scale wells in Hawaii are drilled due to deep water tables in the aquifers, but it is still possible for saltwater intrusion to occur directly through the well opening or downwards along the well (Illangasekare et al., 2006; Inui et al., 2012). Additionally, there is a significant portion of residential wells in Kahului and Kihei–Makena that are shallower and easier for water to infiltrate (Illangasekare et al., 2006), which can lead to a heightened risk of saltwater intrusion in the high well density regions. Based on these factors and the well density map I created, Kahului and Kihei–Makena will be the most vulnerable to saltwater intrusion during major flooding events.

The combined slope and distance from the shore map is an important part of this study because topography determines the extent of tsunami inundation (Kennedy, 2012). Low-lying coastal areas are at a much higher risk for extensive tsunami flooding than high elevation or steep-sloped coastal areas (Klassen & Allen, 2017). A shallow slope and proximity to shore means that water will stay longer and percolate deeper through the surface (Delhi, 2017; Villholth, 2007), further increasing the risk of tsunami-induced saltwater intrusion. Since most of the cities in Maui and the State of Hawaii are located close to the shore and are sitting on low-lying bedrock, it is important for cities to begin thinking about hazard mitigation through infrastructure, technology, and disaster preparedness.

By combining the well density map with the slope and distance from shore map, a more integrated risk assessment is possible since the probability and extent of saltwater intrusion into wells also depend on the slope of the ground and the proximity of wells to the shore. The well density map added to the slope and distance from shore map displayed a higher risk of saltwater intrusion in Kihei–Makena and Kahului in the areas already showing a high risk due to well density (Klassen & Allen, 2017). Since the majority of the well density map was classified as having a low-risk value of one, the overall risk assessment map suggested a low- to moderate risk across most of the island. Realistically, the overall risk in Kahului and Kihei–Makena is more likely to be moderate to high, particularly within the defined flooding zones. The areas with wells that are in low-lying coastal areas are at a heightened risk of saltwater intrusion. This is important for cities to be aware of, as households and businesses may opt to get rid of their private wells in favor of switching to a public water system, which could in turn reduce the magnitude of tsunami-induced saltwater intrusion into the groundwater aquifers that many rely on.

The combined slope and distance from shore map is also important to consider in conjunction with the aquifer and land cover maps. Slope and distance from shore play an important role in determining tsunami-induced saltwater intrusion risk and when those factors are combined with aquifer and land cover types, they provide a more nuanced analysis of how susceptible a region may be to saltwater intrusion (Delhi, 2017; Kennedy, 2012). This is because certain land cover and aquifer types are already vulnerable to saltwater intrusion, so when they exist in a low-lying coastal area, the risk is exacerbated. Overall, overlaying aquifer types and land cover classes with the slope and distance from shore risk map showed that the predominant aquifer and land cover types in the Kahului and Kihei–Makena flooding zones put the regions at risk for tsunami-induced saltwater intrusion.

I found that sedimentary aquifers make up a high percentage within the flooding zones in Kahului and Kihei–Makena which was expected because they formed as a result of the isthmus that connected the East and West Maui volcanoes (Scot Izuka et al., n.d.). These aquifers are sedimentary, unconfined aquifers that are in contact with seawater, while the less frequent aquifers are perched, unconfined, and not in contact with seawater. The types of aquifers present can be a strong indicator of how vulnerable a region may be to tsunami-induced saltwater intrusion since different aquifer characteristics may allow for easier or more frequent infiltration than others (Kennedy, 2012).

I found that in Kahului and Kihei–Makena, sedimentary aquifers are located within the high-risk zones and make up a large percentage of the aquifer type within the flooding zones, while perched aquifers make up a small percentage. The aquifer material is an important determining factor of saltwater intrusion because different materials allow for varying rates of saltwater infiltration. Two studies conducted in Spain and Germany found that among other

factors, different aquifer materials have contributed to varying levels of saltwater intrusion since aquifer types have different permeabilities and conductivities associated with them (Calvache & Pulido-Bosch, 1994; Meyer et al., 2019). In Kahului and Kihei–Makena, the sedimentary aquifers have a lower permeability than the volcanic aquifers that make up the rest of the island. This impedes the recharge and movement of groundwater through the aquifer, which decreases an aquifer's risk of saltwater intrusion through the surface but can limit the aquifer's ability to naturally recover through precipitation events (Scot Izuka et al., n.d.). Perched aquifers make up a smaller percentage of the aquifers within the Kahului and Kihei–Makena flooding zones, but perched aquifers can increase a region's risk for saltwater intrusion since the impermeable layer below the aquifer can limit the amount of infiltration, storage, and recharge (Yousif & Bubenzer, n.d.)

In Kahului and Kihei–Makena, all the aquifers within the flooding zones were unconfined, which have a higher risk of saltwater intrusion during major flooding events. This is because they lack an impermeable layer of sediment above the saturated zone to isolate them from infiltration through the surface, allowing saltwater to infiltrate easily (Adebayo & Abraham, 2018). This in turn means that unconfined aquifers can naturally recover from groundwater salinization quickly since precipitation events can help flush out saltwater if the aquifer does not have a confining layer above it (Şen, 2015). Since Maui has both confined and unconfined aquifers, it is important for Maui to understand the different ways that the two types of aquifers can potentially impact an area's vulnerability to saltwater intrusion during flooding events.

In Kahului and Kihei–Makena, aquifers that are in contact with seawater make up the majority of the aquifer type within the Risk 4 and 5 categories, which increases their

vulnerability to saltwater intrusion. This risk is higher during major flooding events like tsunamis where there is a high volume of water being flooded horizontally and vertically onto land (Adebayo & Abraham, 2018). The lateral intrusion of saltwater is common when an aquifer is in contact with seawater because extensive flooding disturbs the saltwater-freshwater interface in an aquifer, thus leading to saltwater intrusion (Kumaraguru et al., 2007; Liu & Tokunaga, 2019). Although it is not possible to change the aquifer characteristics in Maui, it is useful to know which aquifers make a region more vulnerable to saltwater intrusion so that cities can either switch to relying more on less vulnerable aquifers or put plans in place to remediate salinized groundwater.

Mapping land cover with slope and distance from shore is important when understanding saltwater intrusion because the spatial distribution of different land cover types located in vulnerable flooding zones can determine the extent of infiltration of water into the ground (Klassen & Allen, 2017). Certain land cover types increase a region's risk of saltwater intrusion (AlQattan et al., 2020), and if those land cover types are in low-lying coastal areas the risk is exacerbated due to longer flooding durations and larger volumes of water onshore.

I expected that impervious surfaces would be the largest land cover class within the high-risk, flooding zones because the two study regions, Kahului and Kihei–Makena, were selected for their large populations. In Kahului, I found that impervious surfaces, open water, open space developed, and wetlands had high percentages within the Risk 5 category, but only impervious surfaces and open water were present within the flooding zone in high percentages. In Kihei–Makena, all the land cover types were classified within the Risk 5 category, but similar to Kahului, impervious surfaces and open water made up the majority of the land cover types within the flooding zone.

It is integral to look at the percentage of each land cover type within the flooding zones since different land cover types are more susceptible to saltwater intrusion than others. For example, wetlands are highly susceptible to saltwater intrusion (White & Kaplan, 2017) but take up less than 5% of the total land cover in Kahului and Kihei–Makena which means they will not need to be as worried about wetlands. Alternatively, Maui has seen an increase in impervious surfaces and a reduction in the natural land cover which has altered how susceptible the region may be to saltwater intrusion due to decreased aquifer recharge rates, groundwater elevations, and freshwater heads (AlQattan et al., 2020). Open water on land was present in both Kahului and Kihei–Makena but was not at high risk for saltwater intrusion into aquifers. However, the salinization of surface water can change its chemical and biological properties, which presents additional problems for the ecosystems impacted (White & Kaplan, 2017). Land cover is a feature that could potentially be altered to have a positive impact on tsunami risk though, through activities such as increasing the amount of coastal vegetation to mitigate tsunami wave heights and flooding extents (Carlos et al., 2011; Delhi, 2017).

Overall, I found that Kahului and Kihei–Makena are at high risk for tsunami-induced saltwater intrusion based on the integration of tsunami design zone maps and risk assessment maps. These maps have the potential to become an extremely useful tool for city planners and emergencies response and management teams because it is important for the State of Hawaii and other vulnerable regions to understand how tsunamis will affect their groundwater sources (Tully et al., 2019). Climate change is going to increase the intensity and frequency of tsunamis across the world (Li et al., 2018), which means many coastal communities are going to be at a heightened risk for tsunami-induced saltwater intrusion.

Tsunami-induced saltwater intrusion is a serious issue for many regions, but especially for Hawaii because groundwater makes up 99% of the state's domestic water use. It is used for drinking water, irrigation, and commercial and industrial needs (Gingerich et al., n.d.), so the salinization of major aquifers following a tsunami would have a lasting impact on the island's residents, their agriculture, and economy (Illangasekare et al., 2006; Liu & Tokunaga, 2019; Violette et al., 2009). A couple of countries experienced prolonged periods of salinized groundwater following the 2004 tsunami, due to low precipitation levels and the lack of successful groundwater recovery initiatives (Villholth & International Irrigation Management Institute., 2005; Violette et al., 2009). If Hawaii were to experience an extreme case of tsunami-induced saltwater intrusion, they would need to utilize unaffected aquifers and most likely, import bottled water for drinking. Given that there have been regions whose aquifers have not returned to their normal state for years, it is important for Maui and Hawaii to be aware and prepared. As drinking salinized water is associated with increased rates of cardiovascular diseases, diarrhea, and abdominal pain (Chakraborty et al., 2019), it is integral for the issue of tsunami-induced saltwater intrusion to be properly understood and prepared for.

Future directions

This study evaluated seven factors predicted to influence tsunami-induced saltwater intrusion vulnerability; however, several other possible factors exist that were not considered within the scope of this project. For example, well water elevations are an important indicator of saltwater intrusion risk; if the water is below sea level, for example, an aquifer may be at increased risk of saltwater intrusion (Jasechko et al., 2020). My analysis of aquifer vulnerability to saltwater intrusion in this study was based on studies that provided the relative level of an

aquifer's permeability. In the future, it would be useful to conduct a quantitative analysis that assessed permeability values to incorporate into the relative risk assessment.

The risk assessment maps that I created in this study are intended to serve as a preliminary analysis of tsunami-induced saltwater intrusion risk. Many of the risk values that I assigned to my risk assessment maps were either based on studies that created similar maps or self-defined. This method could have created some biased assessments of risk; accordingly, future work should seek to incorporate empirical data on saltwater intrusion wherever possible in order to develop a less arbitrary risk assessment system.

CONCLUSION

The creation and integration of probabilistic tsunami design zone and risk assessment maps is an important step towards ensuring the safety of coastal groundwater resources for high-risk areas in Maui. Through this study, I have determined that factors including well density, topography, aquifer characteristics, land cover, and tsunami extents are a fundamental part of understanding the vulnerability of certain regions to tsunami-induced saltwater intrusion. Based on the probabilistic tsunami design zone maps and risk assessment maps I created, the census-designated places of Kahului and Kihei–Makena are extremely vulnerable to tsunami-induced saltwater intrusion.

As climate change causes sea levels to rise, there is going to be an increase in the intensity and frequency of tsunamis which will lead to more coastal areas dealing with the long-term effects of tsunami-induced saltwater intrusion. This issue is especially dangerous in Maui and the rest of Hawaii because if the state's aquifers were to become salinized, water availability will become a major issue for the residents of Hawaii. As Hawaii is comprised of islands, aquifer

storage capacity is already limited, and delivering bottled water to residents is more difficult due to their isolated location.

This study seeks to provide an initial risk assessment for Maui and other coastal regions that will likely begin facing issues of saltwater intrusion and tsunami-induced saltwater intrusion. If regions can determine their risk of tsunami-induced saltwater intrusion, they may be able to implement policies and management practice to promote more sustainable aquifer usage, the movement of wells farther from the shore, or the addition of trees or infrastructure near the coast that can limit tsunami run-up. Expanding the use of probabilistic tsunami design zone maps in conjunction with saltwater intrusion risk assessment maps to the rest of Hawaii and more regions across the world can ensure that coastal communities would be more prepared to mitigate and remediate the effects of tsunami-induced saltwater intrusion.

TABLES AND FIGURES

Table 1. The percentage of aquifer types within the flood zones (designated by the probabilistic tsunami design zone maps) and across each risk category generated from the combined slope and distance from shore map, for the Kahului and Kihei–Makena regions.

Region	Aquifer type	% within flood zone	% of aquifer type within each risk class				
			1	2	3	4	5
Kahului	Sedimentary, unconfined, in contact with seawater	77%	0%	1%	3%	25%	71%
	Perched, unconfined, not in contact with seawater	23%	0%	1%	5%	63%	33%
Kihei–Makena	Sedimentary, unconfined, in contact with seawater	95%	0%	1%	3%	13%	82%
	Perched, unconfined, not in contact with seawater	5%	2%	3%	8%	24%	64%

Table 2. Percentage of land cover classes within the flood zones (designated by the probabilistic tsunami design zone maps) and across each risk category generated from the combined slope and distance from shore map, for the Kahului and Kihei–Makena regions.

Region	Land cover class	% within flood zone	% of each land cover type within each risk class				
			1	2	3	4	5
Kahului	Impervious Surface	31%	0%	0%	1%	22%	77%
	Open Space Developed	13%	0%	1%	3%	25%	71%
	Cultivated Land/Pasture/Hay	11%	0%	0%	2%	68%	30%
	Grassland	9%	0%	1%	7%	56%	37%
	Evergreen	7%	0%	2%	8%	27%	63%
	Scrub/Shrub	4%	0%	3%	9%	33%	55%
	Wetlands	4%	0%	2%	6%	20%	72%
	Unconsolidated Shore	1%	0%	1%	7%	32%	60%
	Bare Land	2%	0%	2%	8%	44%	45%
	Open Water	18%	0%	1%	4%	12%	83%
Kihei–Makena	Impervious Surface	29%	0%	1%	2%	11%	87%
	Open Space Developed	14%	0%	1%	4%	15%	80%
	Cultivated Land/Pasture/Hay	1%	0%	1%	3%	5%	91%
	Grassland	6%	0%	1%	5%	18%	75%
	Evergreen	13%	0%	1%	5%	16%	78%
	Scrub/Shrub	5%	0%	1%	5%	18%	75%
	Wetlands	0%	0%	0%	1%	14%	85%
	Unconsolidated Shore	1%	0%	0%	1%	15%	84%
	Bare Land	2%	0%	2%	7%	21%	70%
	Open Water	30%	0%	1%	4%	20%	75%

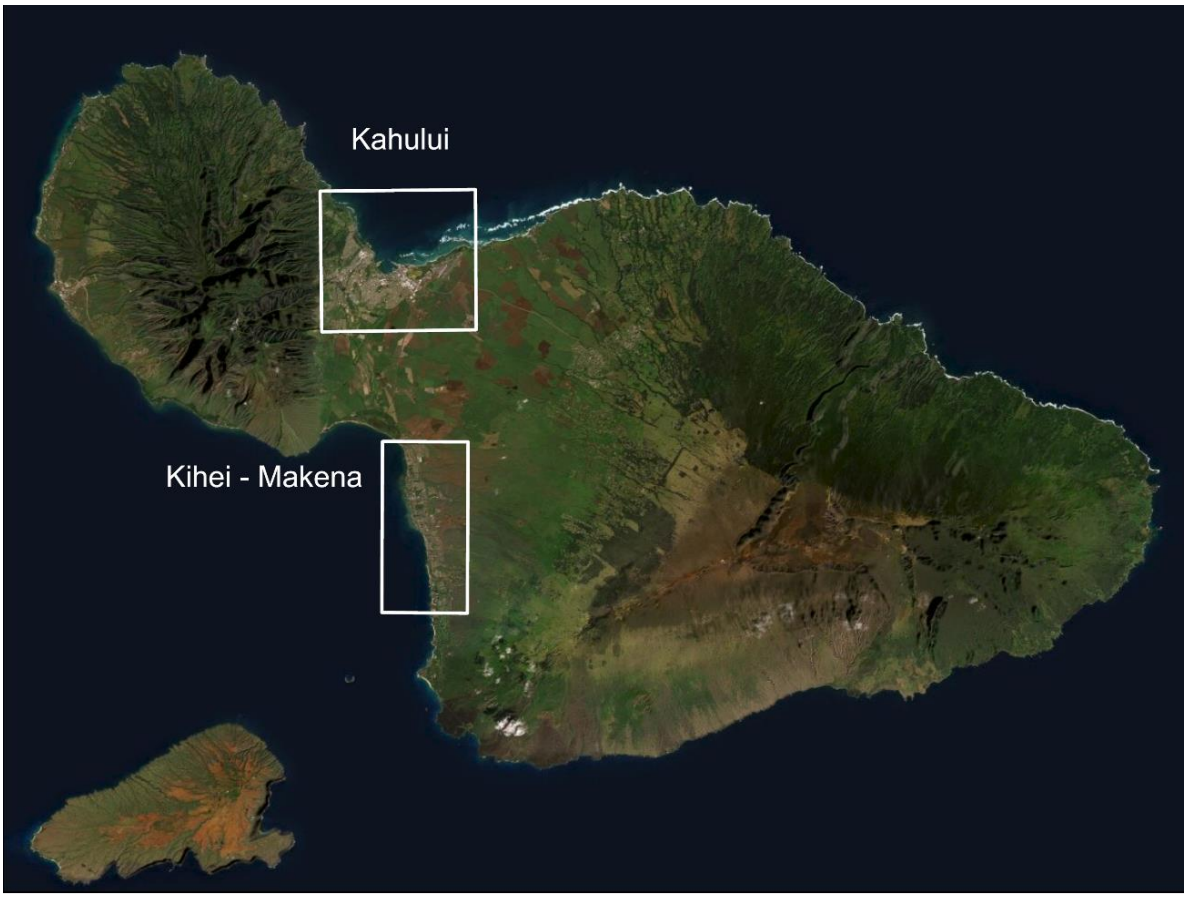

Figure 1. Study regions on Maui, Hawaii, USA: Kahului and Kihei–Makena.

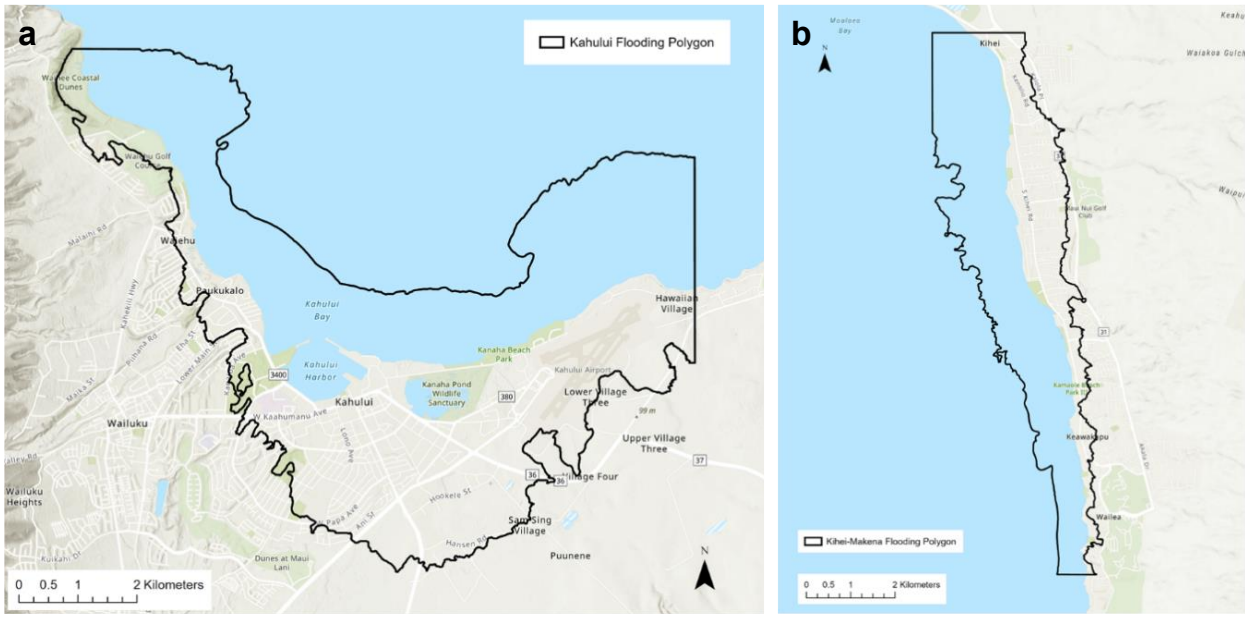

Figure 2. Flooding polygons representing the probabilistic maximum flooding extents for the (a) Kahului; and (b) Kihei–Makena study regions on Maui, Hawaii, USA.

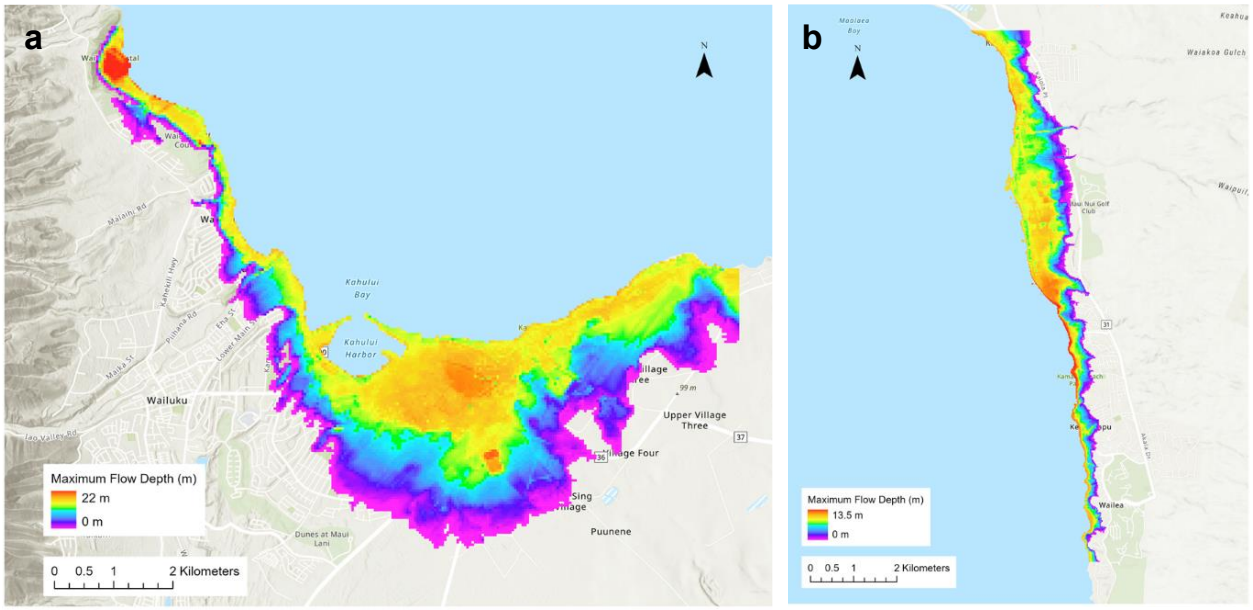

Figure 3. Maximum flooding extent maps depicting maximum flow depths, in meters, for the (a) Kahului; and (b) Kihei–Makena study regions.

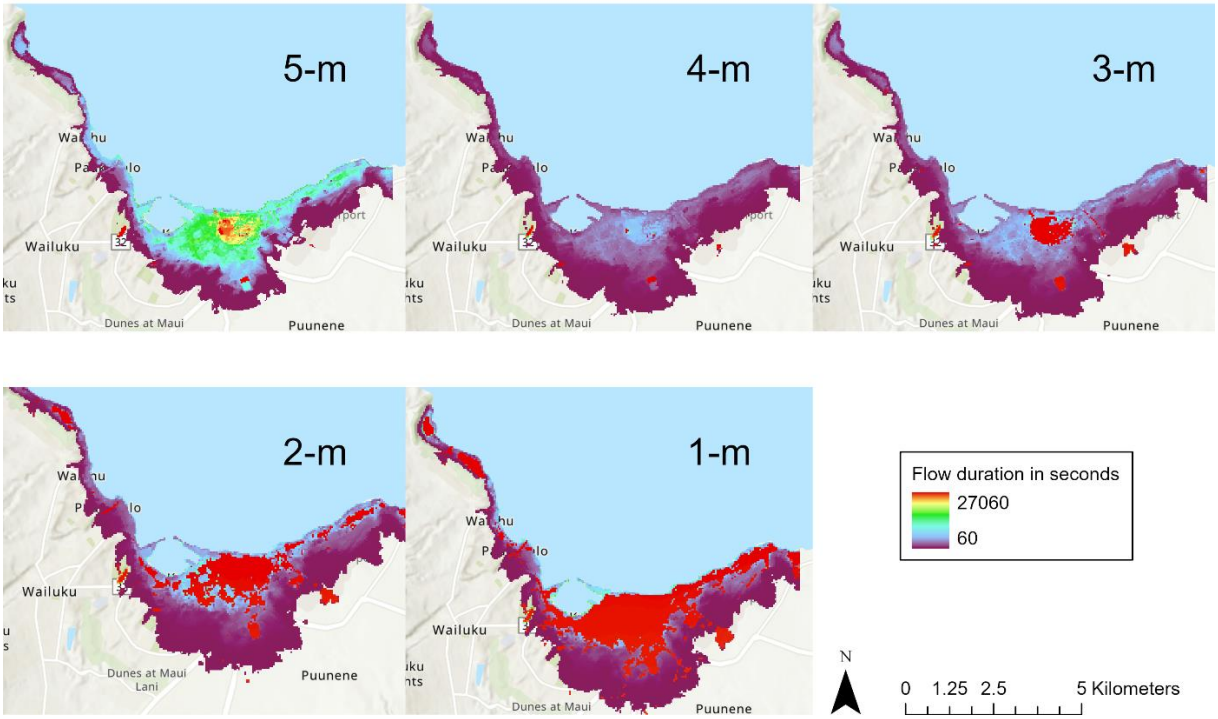

Figure 4. Flow duration, in seconds, for the Kahului study region. Flow duration was calculated at or above a water depth of 5-meters, 4-meters, 3-meters, 2-meters, and 1-meter.

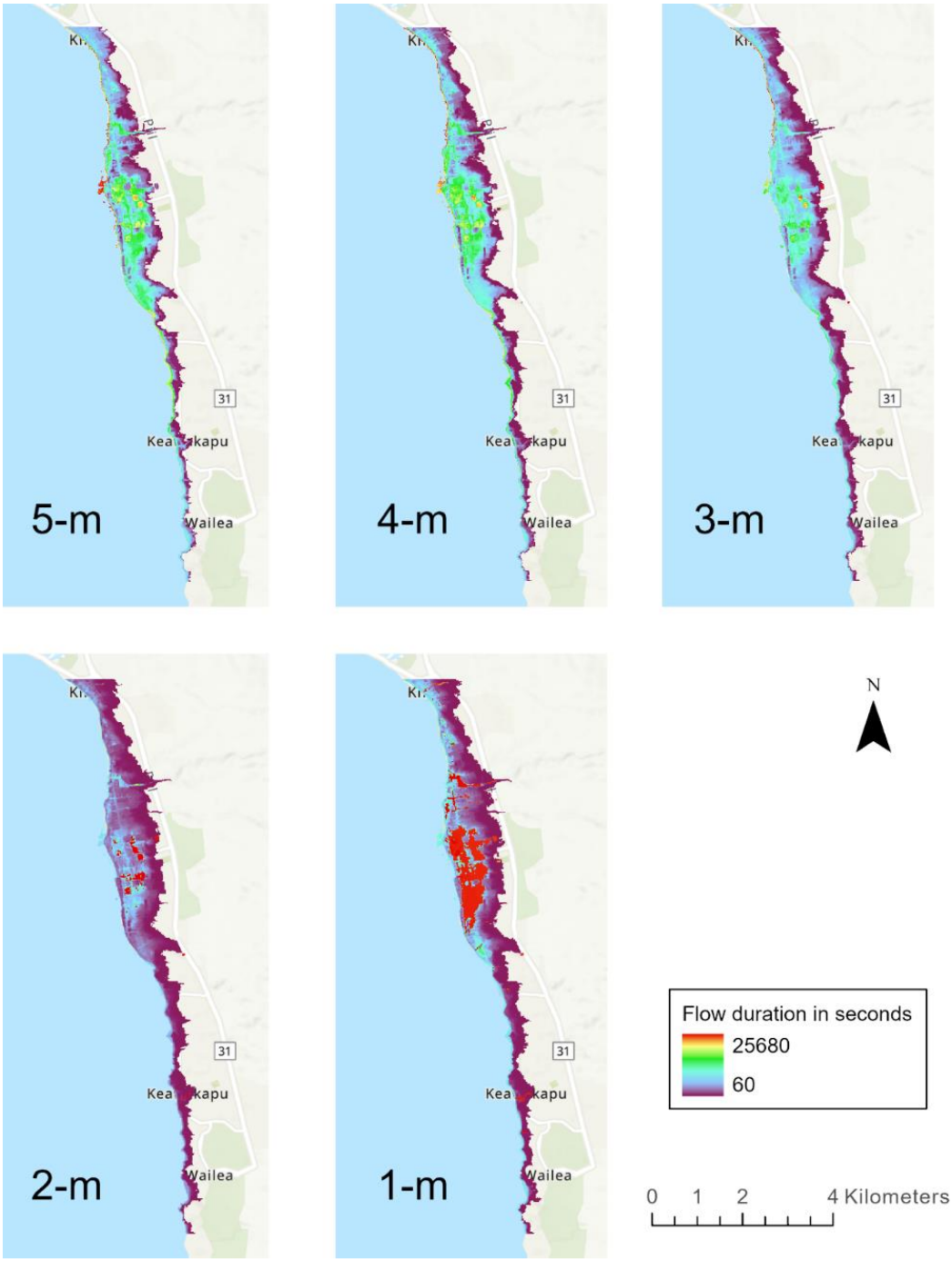

Figure 5. Flow duration, in seconds, for the Kihei–Makena study region. Flow duration was calculated at or above a water depth of 5-meters, 4-meters, 3-meters, 2-meters, and 1-meter.

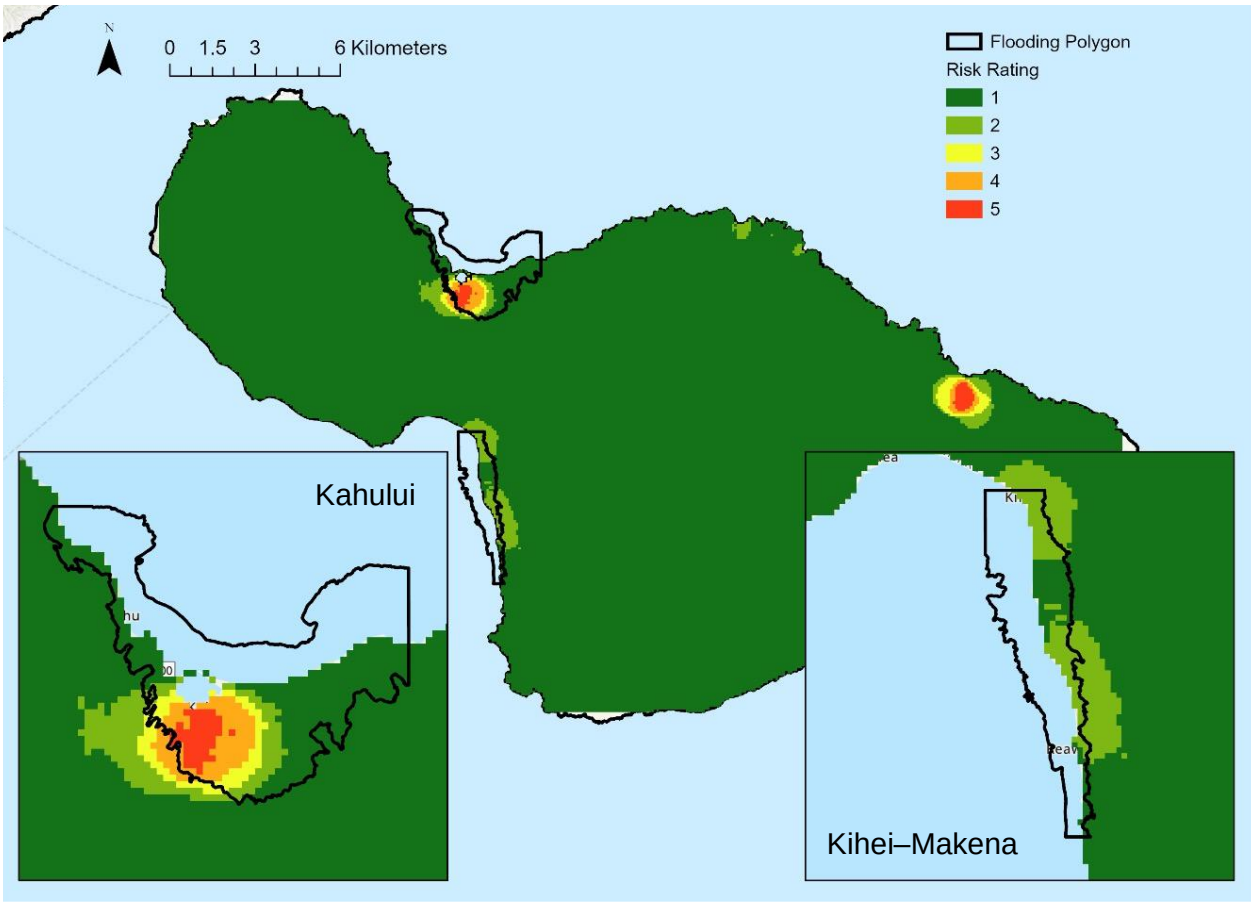

Figure 6. Relative saltwater intrusion risk, ranging from 1–5, based on well density (well densities associated with each risk class are defined in Table A1). Risk for the Kahului study region is shown in the bottom left corner, and risk for the Kihei–Makena study region is shown in the bottom right corner.

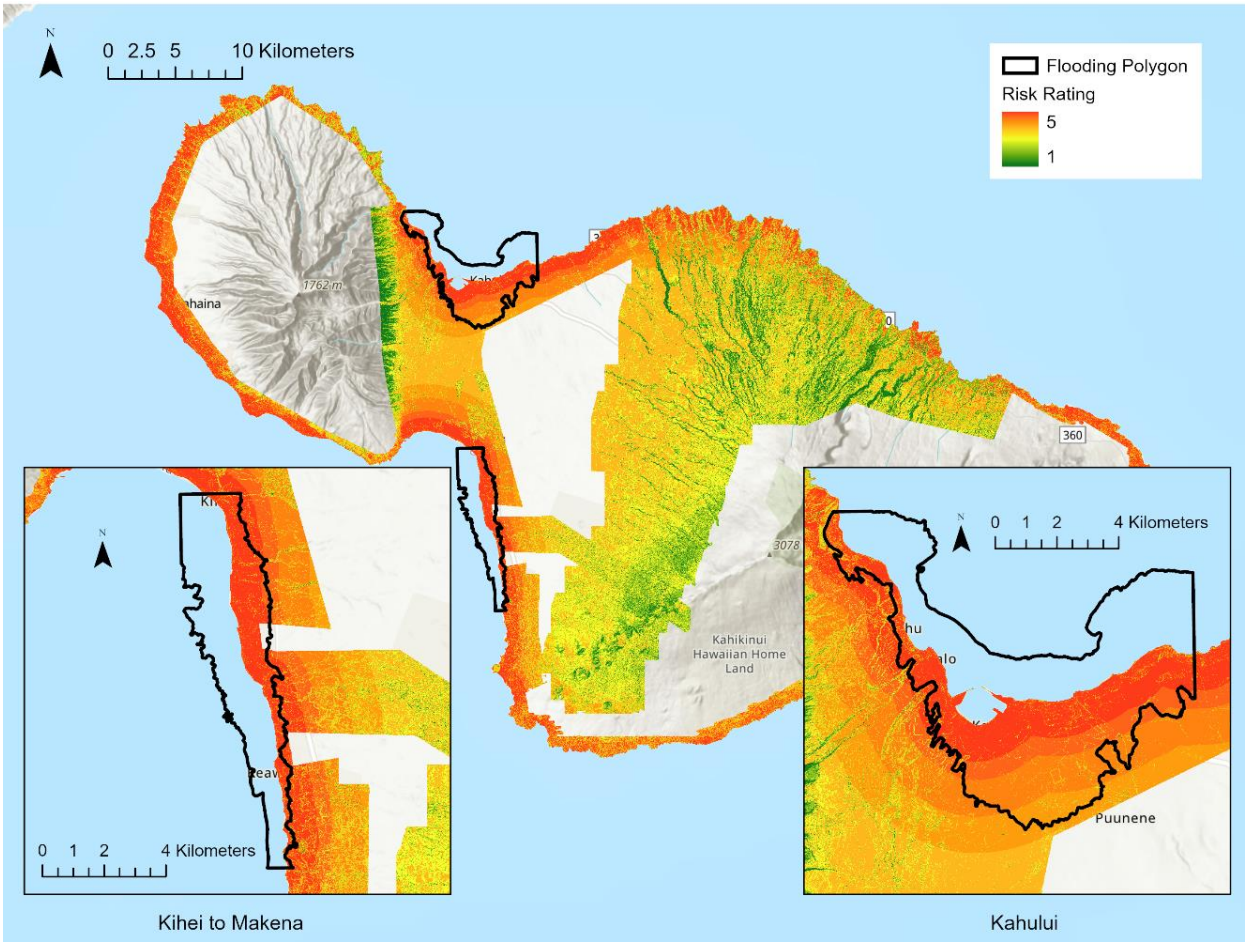

Figure 7. Relative saltwater intrusion risk, ranging from 1–5, based on combined slope and distance from shore. Overall risk across is displayed for the island of Maui, Hawaii (where data was available), as well as for the Kihei–Makena (lower-left) and Kahului (lower-right) study regions. Risk classes are displayed across a color-gradient ranging from low risk (green) to high risk (red).

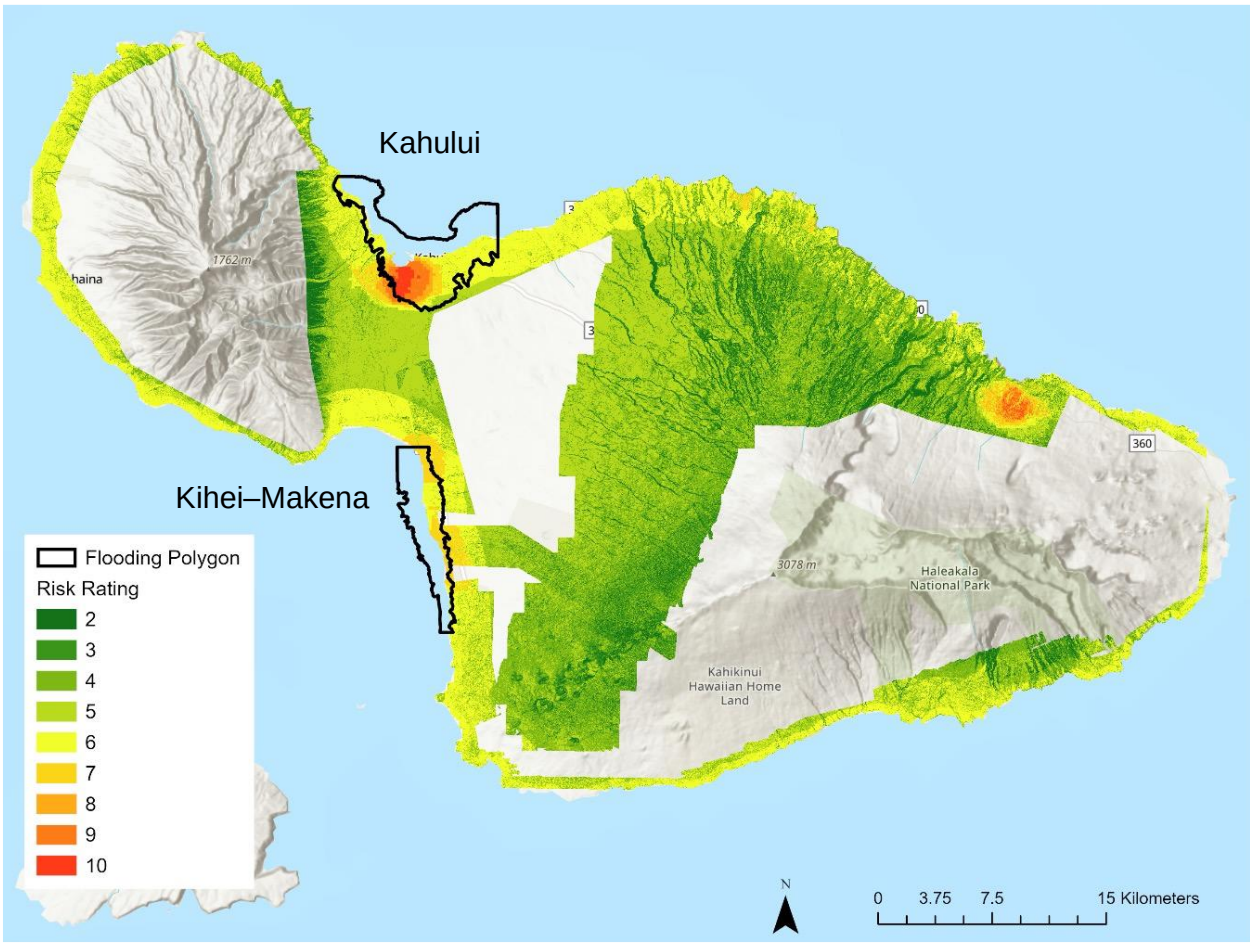

Figure 8. Overall risk of saltwater intrusion, ranging from 2–10, based on the sum of the well density layer and combined slope + distance from shore layer. Risk is displayed for the island of Maui, Hawaii (where data was available), with the flooding polygons outlined for each study region.

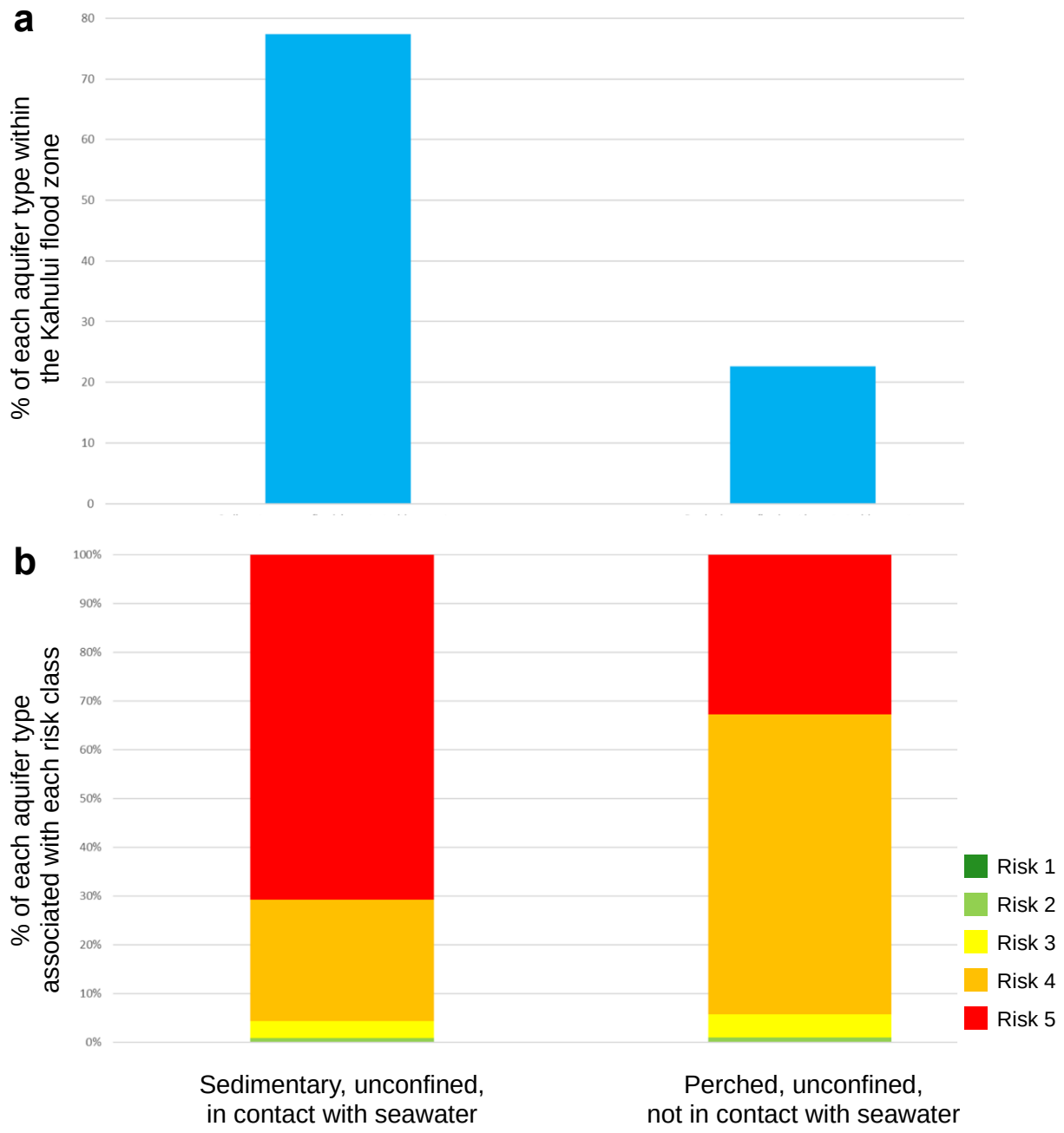

Figure 9. Stacked bar graphs for Kahului representing (a) the percentage of each aquifer type within the Kahului flooding zone polygon; and (b) the percentage of each aquifer type associated with each risk class, 1–5.

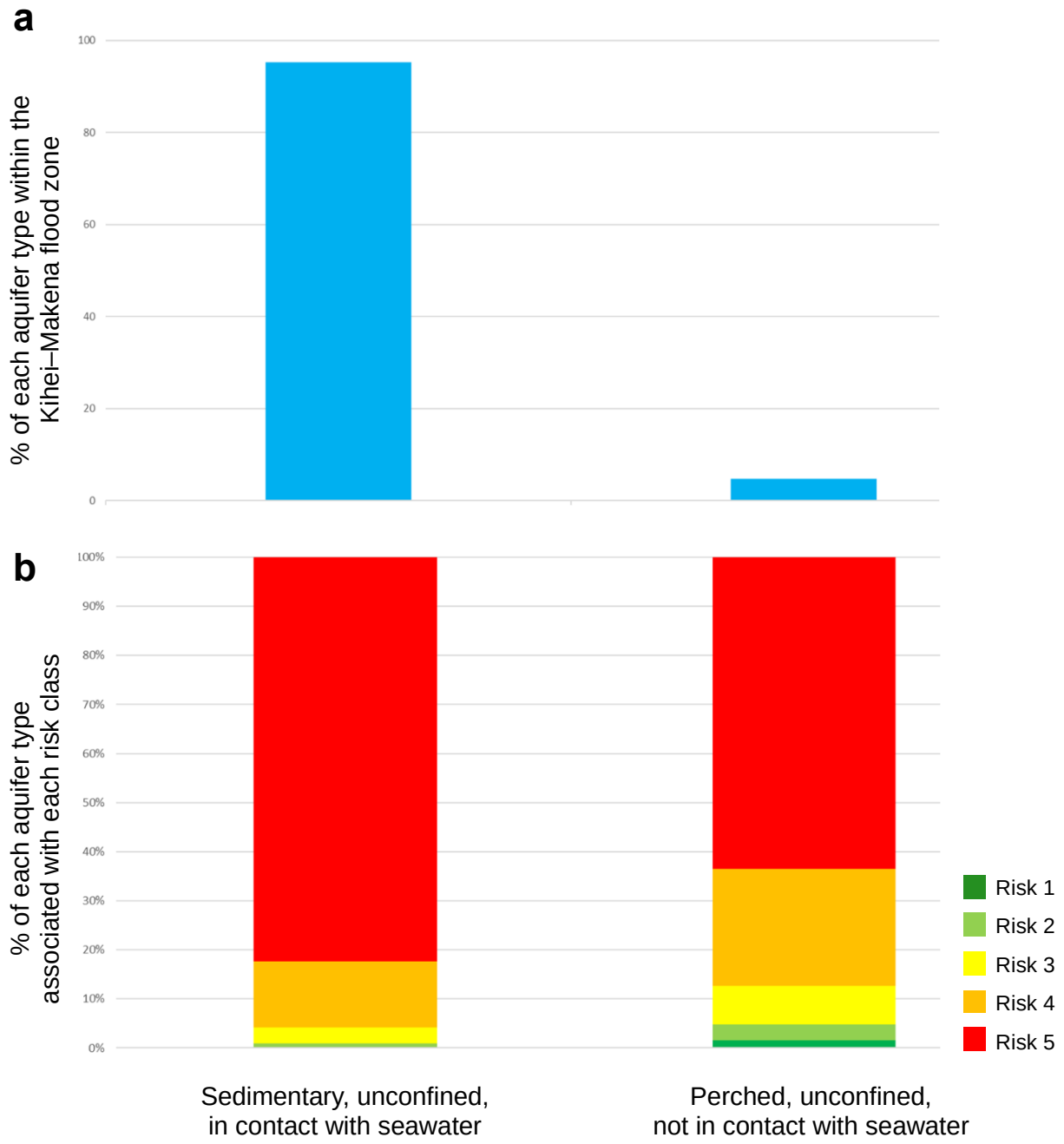

Figure 10. Stacked bar graphs for Kihei–Makena representing (a) the percentage of each aquifer type within the Kihei–Makena flooding zone polygon; and (b) the percentage of each aquifer type associated with each risk class, 1–5.

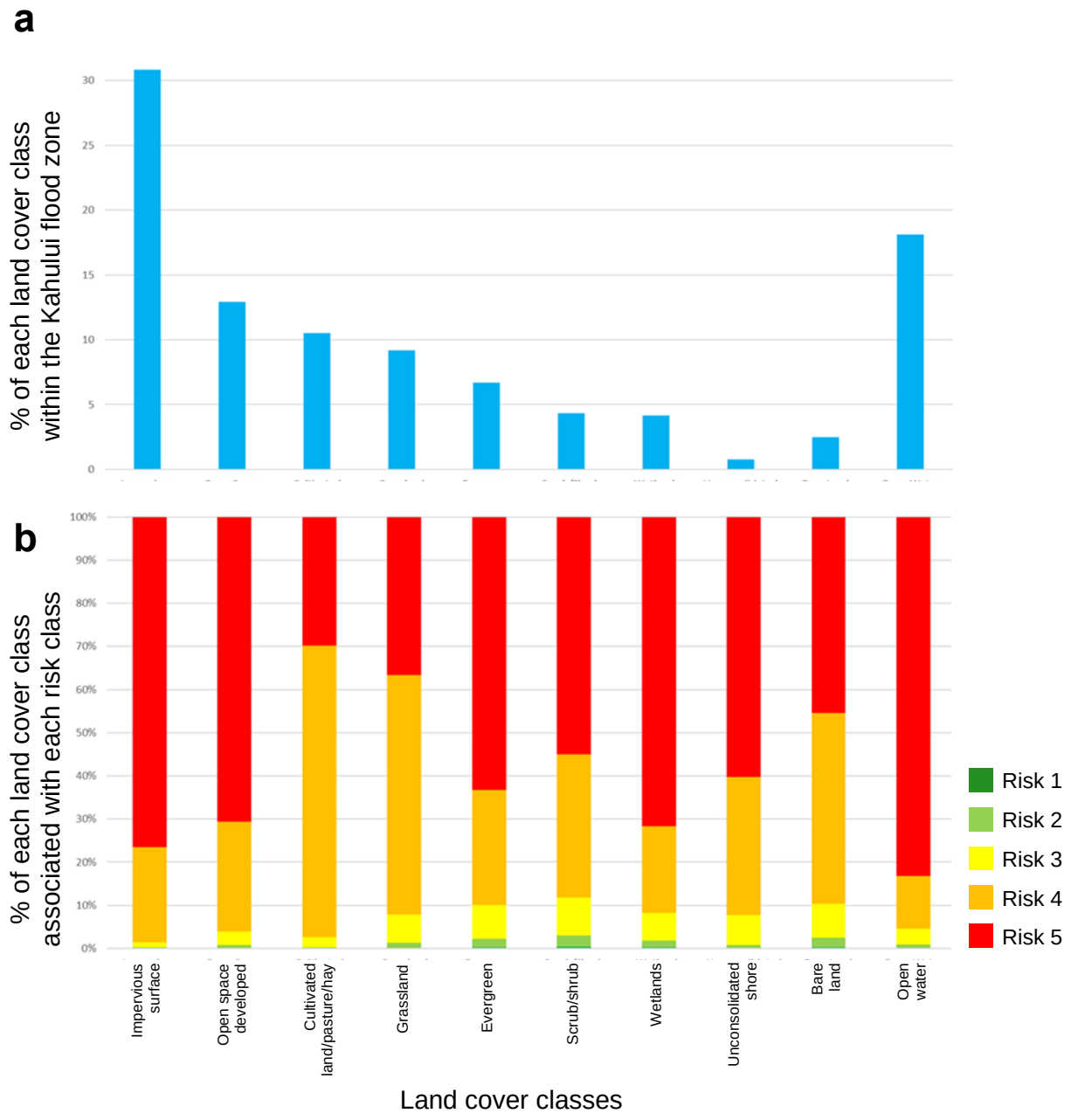

Figure 11. Stacked bar graphs for Kahului representing (a) the percentage of each land cover class within the Kahului flooding zone polygon; and (b) the percentage of each land cover class associated with each risk class, 1–5.

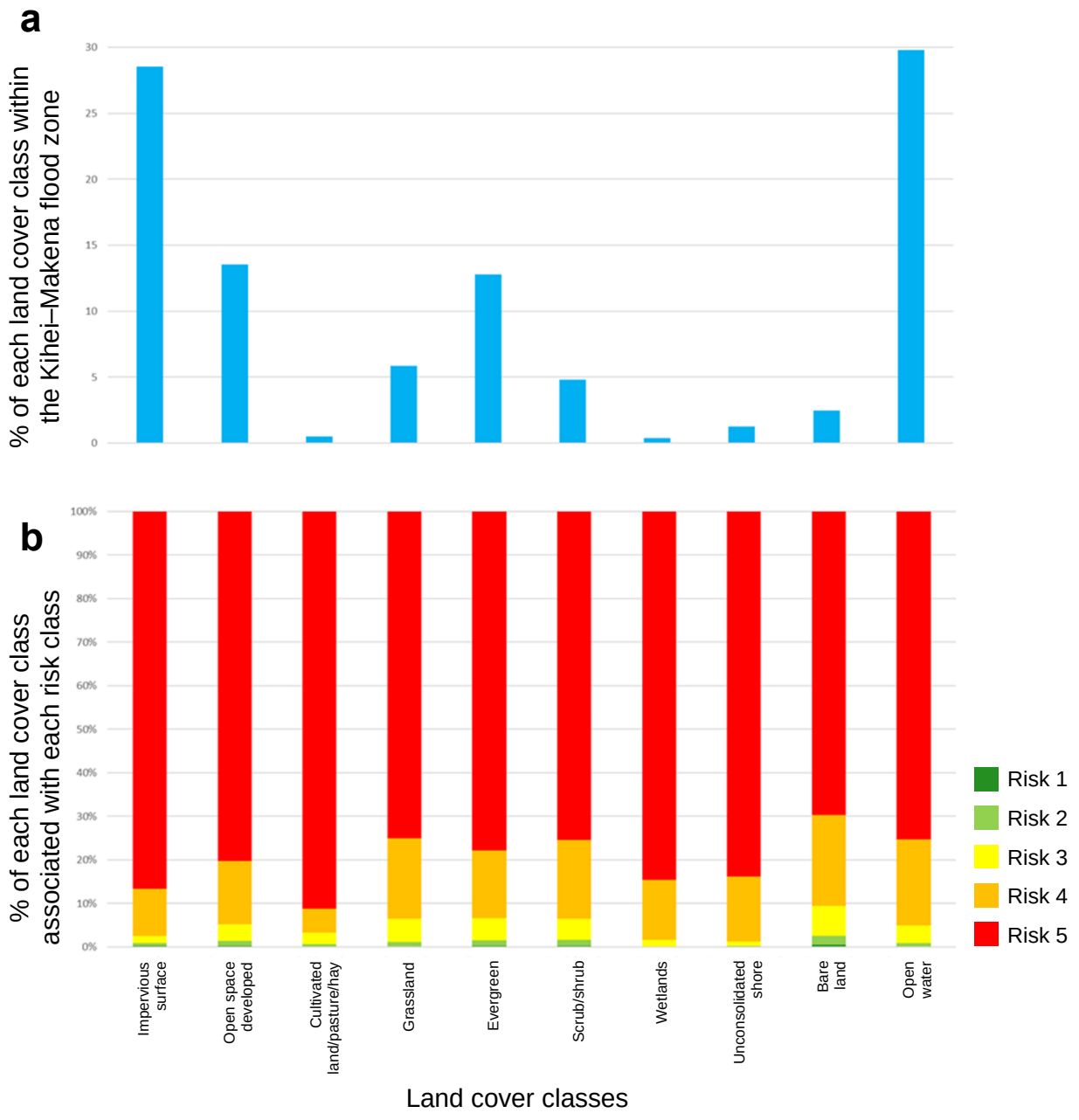

Figure 12. Stacked bar graphs for Kihei–Makena representing (a) the percentage of each land cover class within the Kihei–Makena flooding zone polygon; and (b) the percentage of each land cover class associated with each risk class, 1–5.

REFERENCES

Adebayo, S., & Abraham, A. (2018). Aquifer, Classification and Characterization. In *Aquifers - Matrix and Fluids*. InTech. https://doi.org/10.5772/intechopen.72692

Alexander, M. A., Scott, J. D., Friedland, K. D., Mills, K. E., Nye, J. A., Pershing, A. J., & Thomas, A. C. (2018). Projected sea surface temperatures over the 21st century: Changes in the mean, variability and extremes for large marine ecosystem regions of Northern Oceans. In *Elementa* (Vol. 6). University of California Press. https://doi.org/10.1525/elementa.191

AlQattan, N., Acheampong, M., Jaward, F. M., Vijayakumar, N., & Enomah, L. E. D. (2020). Evaluation of the potential hydrological impacts of land use/cover change dynamics in Ghana's oil city. *Environment, Development and Sustainability*, *22*(8), 7313–7330. https://doi.org/10.1007/s10668-019-00507-0

American Society of Civil Engineers (2017), Minimum design loads and associated criteria for building and other structures (ASCE Standard – ASCE/SEI 7-16) provisions and commentary 2-book set, published by American Society of Civil Engineers.

American Society of Civil Engineers (2022), Minimum design loads and associated criteria for building and other structures (ASCE/SEI 7-22) provisions and commentary 2-book set, doi:10.1061/9780784415788, published by American Society of Civil Engineers.

Angove, M., L. Kozlosky, P. Chu, G. Dusek, G. Mann, E. Anderson, J. Gridley, D. Arcas, V. Titov, M. Eble, K. McMahon, B. Hirsch, and W. Zaleski (2021): Addressing the meteotsunami risk in the United States. Nat. Hazards, doi: 10.1007/s11069-020-04499-3.

Benevolenza, M. A., & Derigne, L. (2018). *Journal of Human Behavior in the Social Environment The impact of climate change and natural disasters on vulnerable*

populations: A systematic review of literature. https://doi.org/10.1080/10911359.2018.1527739

Bernard, E., & Titov, V. (2015). Evolution of tsunami warning systems and products. In *Philosophical Transactions of the Royal Society A: Mathematical, Physical and Engineering Sciences* (Vol. 373, Issue 2053). Royal Society of London. https://doi.org/10.1098/rsta.2014.0371

Calvache, M. L., & Pulido-Bosch, A. (1994). Modeling the Effects of Salt-Water Intrusion Dynamics for a Coastal Karstified Block Connected to a Detrital Aquifer. *Groundwater, 32*(5), 767–777. https://doi.org/10.1111/J.1745-6584.1994.TB00918.X

Carlos, J., Bayas, L., Marohn, C., Dercon, G., Dewi, S., Piepho, H. P., Joshi, L., van Noordwijk, M., & Cadisch, G. (2011). *Influence of coastal vegetation on the 2004 tsunami wave impact in west Aceh*. *108*(46), 18612–18617. https://doi.org/10.1073/pnas.1013516108/-/DCSupplemental

Cerizo, K. (n.d.). *Maui County drought conditions worst in state | News, Sports, Jobs - Maui News*. Retrieved March 28, 2022, from https://www.mauinews.com/news/local-news/2021/10/maui-county-drought-conditions-worst-in-state/

Cerizo, K. (2022). *Drought returns to Maui County during 'strange' wet season | Maui Now*. https://mauinow.com/2022/02/04/drought-returns-to-maui-county-during-strange-wet-season/

Chock, G.Y.K., L. Carden, I. Robertson, Y. Wei, R. Wilson, and J. Hooper (2018): Tsunami resilient building design considerations for coastal communities of Washington, Oregon, and California. J. Struct. Eng., 144(8), 04018116, doi: 10.1061/(ASCE)ST.1943-541X.0002068.

Chock, S.E., I. Robertson, D. Kriebel, M. Francis, and I. Nistor (2013), Tohoku, Japan, Earthquake and Tsunami of 2011: Performance of Structures Under Tsunami Loads, https://doi.org/10.1061/9780784412497, 2013 American Society of Civil Engineers.

Chakraborty, R., Khan, K. M., Dibaba, D. T., Khan, M. A., Ahmed, A., & Islam, M. Z. (2019). Health implications of drinking water salinity in coastal areas of Bangladesh. *International Journal of Environmental Research and Public Health*, *16*(19). https://doi.org/10.3390/IJERPH16193746

Climate of Hawai`i. (n.d.). Retrieved February 3, 2022, from https://www.weather.gov/hfo/climate_summary

Delhi, N. (2017). *Government of India Ministry of Water Resources, River Development & Ganga Rejuvenation Problems of Salination of Land in Coastal Areas of India and Suitable Protection Measures Hydrological Studies Organization Central Water Commission*.

Dura, T., Garner, A. J., Weiss, R., Kopp, R. E., Engelhart, S. E., Witter, R. C., Briggs, R. W., Mueller, C. S., Nelson, A. R., & Horton, B. P. (2021). Changing impacts of Alaska-Aleutian subduction zone tsunamis in California under future sea-level rise. *Nature Communications*, *12*(1). https://doi.org/10.1038/s41467-021-27445-8

Firing, Y. L., & Merrifield, M. A. (2004). Extreme sea level events at Hawaii: Influence of mesoscale eddies. *Geophys. Res. Lett, 31*, 24306. https://doi.org/10.1029/2004GL021539

Giambelluca, T. W., thomas Giambelluca, by W., chen, Q., Frazier, abby G., Price, J. P., chen, yi-lenG, chu, P., eischeid, J. K., & delParte, donna. (n.d.). *MARCH 2013 AMERICAN METEOROLOGICAL SOCIETY ON THE WEB ONLINE RAINFALL ATLAS OF HAWAI'I*. https://doi.org/10.1175/BAMS-D-11-00228.1

Gingerich, S. B., Oki, D. S., & Geological Survey, U. (n.d.). *Ground Water in Hawaii*. http://hi.water.usgs.gov

Gonzalez, F. I. (1999). TSUNAMI! *Scientific America*, *280*, 56–65. https://doi.org/10.2307/26058242

Hawai'i State Water Wells - Hawai'i Groundwater & Geothermal Resources Center. (n.d.). Retrieved February 24, 2022, from https://www.higp.hawaii.edu/hggrc/projects/hawaii-state-waterwells/

Hulick, K. (2016). *THE RING OF FIRE: *. https://eds-p-ebscohost-com.coloradocollege.idm.oclc.org/eds/detail/detail?vid=5&sid=0225d823-412f-461a-92c5-aa39f1aa87f1%40redis&bdata=JnNpdGU9ZWRzLWxpdmU%3d#db=pwh&AN=111547248

Illangasekare, T., Tyler, S. W., Clement, T. P., Villholth, K. G., Perera, A. P. G. R. L., Obeysekera, J., Gunatilaka, A., Panabokke, C. R., Hyndman, D. W., Cunningham, K. J., Kaluarachchi, J. J., Yeh, W. W. G., van Genuchten, M. T., & Jensen, K. (2006). Impacts of the 2004 tsunami on groundwater resources in Sri Lanka. *Water Resources Research*, *42*(5). https://doi.org/10.1029/2006WR004876

Inui, T., Yasutaka, T., Endo, K., & Katsumi, T. (2012). Geo-environmental issues induced by the 2011 off the Pacific Coast of Tohoku Earthquake and tsunami. *Soils and Foundations*, *52*(5), 856–871. https://doi.org/10.1016/j.sandf.2012.11.008

Jasechko, S., Perrone, D., Seybold, H., Fan, Y., & Kirchner, J. W. (2020). Groundwater level observations in 250,000 coastal US wells reveal scope of potential seawater intrusion. *Nature Communications*, *11*(1). https://doi.org/10.1038/s41467-020-17038-2

Kaihotsu, I., Onodera, S. ichi, Shimada, J., & Nakagawa, K. (2017). Recovery of groundwater in the Sanriku region contaminated by the tsunami inundation from the 2011 Tohoku earthquake. *Environmental Earth Sciences*, *76*(6). https://doi.org/10.1007/s12665-017-6569-x

Kennedy, G. W. (2012). *DEVELOPMENT OF A GIS-BASED APPROACH FOR THE ASSESSMENT OF RELATIVE SEAWATER INTRUSION VULNERABILITY IN NOVA SCOTIA, CANADA*.

Klassen, J., & Allen, D. M. (2017). Assessing the risk of saltwater intrusion in coastal aquifers. *Journal of Hydrology*, *551*, 730–745. https://doi.org/10.1016/j.jhydrol.2017.02.044

Kumaraguru, A., Wilson, J., Marimuthu, N., & Muthiah, R. C. (2007). *TSUNAMI OF 2004 AND CORAL REEF ENVIRONMENT OF THE SOUTHEAST COAST OF INDIA Coral reef community and spatial cover-Multivariate approach View project Fishery Management View project*. https://www.researchgate.net/publication/235407231

Li, L., Switzer, A. D., Wang, Y., Chan, C.-H., Qiu, Q., & Weiss, R. (2018). A modest 0.5-m rise in sea level will double the tsunami hazard in Macau. In *Sci. Adv* (Vol. 4). https://www.science.org

Liu, J., & Tokunaga, T. (2019). Future Risks of Tsunami-Induced Seawater Intrusion Into Unconfined Coastal Aquifers: Insights From Numerical Simulations at Niijima Island, Japan. *Water Resources Research*, *55*(12), 10082–10104. https://doi.org/10.1029/2019WR025386

Macdonald, G. A., Shepard, F. P., & Cox, D. C. (1946). *The Tsunami of April 1, 1946, in the Hawaiian Islands*.

Merati, N., Chamberlin, C., Moore, C., Titov, V., & Vance, T. C. (2009). Integration of Tsunami Analysis Tools into a GIS Workspace – Research, Modeling, and Hazard Mitigation efforts Within NOAA's Center for Tsunami Research. *Geospatial Techniques in Urban Hazard and Disaster Analysis*, 273–294. https://doi.org/10.1007/978-90-481-2238-7_14

Meyer, R., Engesgaard, P., & Sonnenborg, T. O. (2019). Origin and Dynamics of Saltwater Intrusion in a Regional Aquifer: Combining 3-D Saltwater Modeling With Geophysical and Geochemical Data. *Water Resources Research*, *55*(3), 1792–1813. https://doi.org/10.1029/2018WR023624

Mimura, N. (2013). *Sea-level rise caused by climate change and its implications for society*. *89*, 281–301.

Mink, J. F., & Lau, L. S. (1992). *REPORT DOCUMENTATION FORM Aquifer identification and classification for Kauai: Groundwater protection strategy for Hawaii*.

Pezza, D. A., & White, J. M. (2021). Impact of the Duration of Coastal Flooding on Infrastructure. *Public Works Management and Policy*, *26*(2), 144–163. https://doi.org/10.1177/1087724X20915918

Robertson. (2020a). *Development of High Resolution Probabilistic Tsunami Design Zone Maps Compatible with ASCE 7-22 for Higher-risk Coastal Areas of the Island of Maui-Phase I, State of Hawai'i High-Resolution Inundation Modeling Using MOST*.

Robertson. (2020b). *Tsunami Design Zone Maps for Maui Island-Phase I Report 2. Data Products*.

Scot Izuka, B. K., Engott, J. A., Rotzoll, K., Bassiouni, M., Johnson, A. G., Miller, L. D., & Mair, A. (2015). *Scientific Investigations Report 2015-5164 Volcanic Aquifers of Hawai'i-Hydrogeology, Water Budgets, and Conceptual Models*.

Scot Izuka, B. K., Rotzoll, K., & Nishikawa, T. (n.d.). *Volcanic Aquifers of Hawai'i-Construction and Calibration of Numerical Models for Assessing Groundwater Availability on Kaua'i, O'ahu, and Maui men20-4007_fig00 Kaua'i O'ahu Maui Scientific Investigations Report 2020-5126*.

Şen, Z. (2015). Unconfined Aquifers. In *Practical and Applied Hydrogeology* (pp. 209–278). Elsevier. https://doi.org/10.1016/b978-0-12-800075-5.00004-2

Sepúlveda, I., Haase, J. S., Liu, P. L. F., Grigoriu, M., & Winckler, P. (2021). Non-Stationary Probabilistic Tsunami Hazard Assessments Incorporating Climate-Change-Driven Sea Level Rise. *Earth's Future*, *9*(6). https://doi.org/10.1029/2021EF002007

State of Hawai'i - Hazard Mitigation Plan. (2018).

Swapna, P., Ravichandran, M., Nidheesh, G., Jyoti, J., Sandeep, N., & Deepa, J. S. (2020). Sea-Level Rise. *Assessment of Climate Change over the Indian Region: A Report of the Ministry of Earth Sciences (MoES), Government of India*, 175–189. https://doi.org/10.1007/978-981-15-4327-2_9

Tang, L., V.V. Titov, E. Bernard, Y. Wei, C. Chamberlin, J.C. Newman, H. Mofjeld, D. Arcas, M. Eble, C. Moore, B. Uslu, C. Pells, M.C. Spillane, L.M. Wright, and E. Gica (2012): Direct energy estimation of the 2011 Japan tsunami using deep-ocean pressure measurements. J. Geophys. Res., 117, C08008, doi: 10.1029/2011JC007635.

Tang, L., V. V. Titov, and C. D. Chamberlin (2009), Development, testing, and applications of site-specific tsunami inundation models for real-time forecasting, J. Geophys. Res., 114, C12025, doi:10.1029/2009JC005476.

Thio, H.K., Somerville, P. and Polet, J. (2010), *Probabilistic tsunami hazard in California*, PEER report 2010.108, Pacific Earthquake Engineering Research Center, College of Engineering, University of California, Berkeley.

Titov, V.V. (2009): Tsunami forecasting. Chapter 12 in *The Sea, Volume 15: Tsunamis*, Harvard University Press, Cambridge, MA and London, England, 371–400.

Titov, V.V., A.B. Rabinovich, H.O. Mofjeld, R.E. Thomson, and F.I. González (2005): The global reach of the 26 December 2004 Sumatra Tsunami. Science, 309(5743), 2045–2048.

Tully, K., Gedan, K., Epanchin-Niell, R., Strong, A., Bernhardt, E. S., Bendor, T., Mitchell, M., Kominoski, J., Jordan, T. E., Neubauer, S. C., & Weston, N. B. (2019). The Invisible Flood: The Chemistry, Ecology, and Social Implications of Coastal Saltwater Intrusion. *BioScience*, *368*(5). https://doi.org/10.1093/biosci/biz027

USA: First American state declares a climate emergency - Climate Emergency Declaration. (2021, May 6). https://climateemergencydeclaration.org/usa-first-american-state-declares-a-climate-emergency/

Villholth, K. G. (2007). *Tsunami impacts on groundwater and water supply in eastern Sri Lanka*. *26*(1), 1–11.

Villholth, K. G., & International Irrigation Management Institute. (2005). *Tsunami impacts on shallow groundwater and associated water supply on the East Coast of Sri Lanka : a post-tsunami well recovery support initiative and an assessment of groundwater salinity in three areas of Batticaloa and Ampara Districts*. International Water Management Institute.

Violette, S., Boulicot, G., & Gorelick, S. M. (2009). Tsunami-induced groundwater salinization in southeastern India. *Comptes Rendus - Geoscience*, *341*(4), 339–346. https://doi.org/10.1016/j.crte.2008.11.013

Wei, Y., E. Bernard, L. Tang, R. Weiss, V. Titov, C. Moore, M. Spillane, M. Hopkins, and U. Kânoğlu (2008): Real-time experimental forecast of the Peruvian tsunami of August 2007 for U.S. coastlines. *Geophys. Res. Lett.*, *35*, L04609, doi: 10.1029/2007GL032250.

Wei, Y., C. Chamberlin, V. Titov, L. Tang, and E.N. Bernard (2013): Modeling of the 2011 Japan tsunami - Lessons for near-field forecast. Pure Appl. Geophys., 170(6–8), doi: 10.1007/s00024-012-0519-z, 1309–1331.

Wei, Y., H.K. Thio, G. Chock, V. Titov, and C. Moore (2015): Development of probabilistic tsunami design maps along the U.S. West Coast for ASCE7. In 11th Canadian Conference on Earthquake Engineering, Victoria, BC, 21–24 July 2015.

White, E., & Kaplan, D. (2017). *Ecosystem Health and Sustainability*. https://doi.org/10.1002/ehs2.1258

Yamazaki, Y., Cheung, K.F., and Kowalik, Z. (2011a). Depth-integrated, non-hydrostatic model with grid nesting for tsunami generation, propagation, and run-up. *International Journal for Numerical Methods in Fluids*, 67(12), 2081-2107.

Yavuz, C., Kentel, E., & Aral, M. M. (2020). *Climate Change Risk Evaluation of Tsunami Hazards in the Eastern Mediterranean Sea*. 1–18. https://doi.org/10.3390/w12102881

Yousif, M., & Bubenzer, O. (n.d.). *Perched groundwater at the northwestern coast of Egypt: a case study of the Fuka Basin*. https://doi.org/10.1007/s13201-011-0023-0

APPENDICES

Table A1. Ranges of well densities (represented by the number of wells per hectare), slopes (in degrees), and distance from shore (in meters) associated with each relative risk class. Relative risk ranges from 1 to 5, with 1 representing of the lowest risk of saltwater intrusion and 5 representing the highest saltwater intrusion risk. Risk classes were assigned using the "equal intervals" data classification in ArcGIS Pro.

Risk class	Well density (# of wells/ha)	Slope (degrees)	Distance from shore (meters)
1	0–3	72–90°	2500 m
2	3–6	54–72°	1500 m
3	6–9	36–54°	1000 m
4	9–12	18–36°	500 m
5	>12	0–18°	0 m

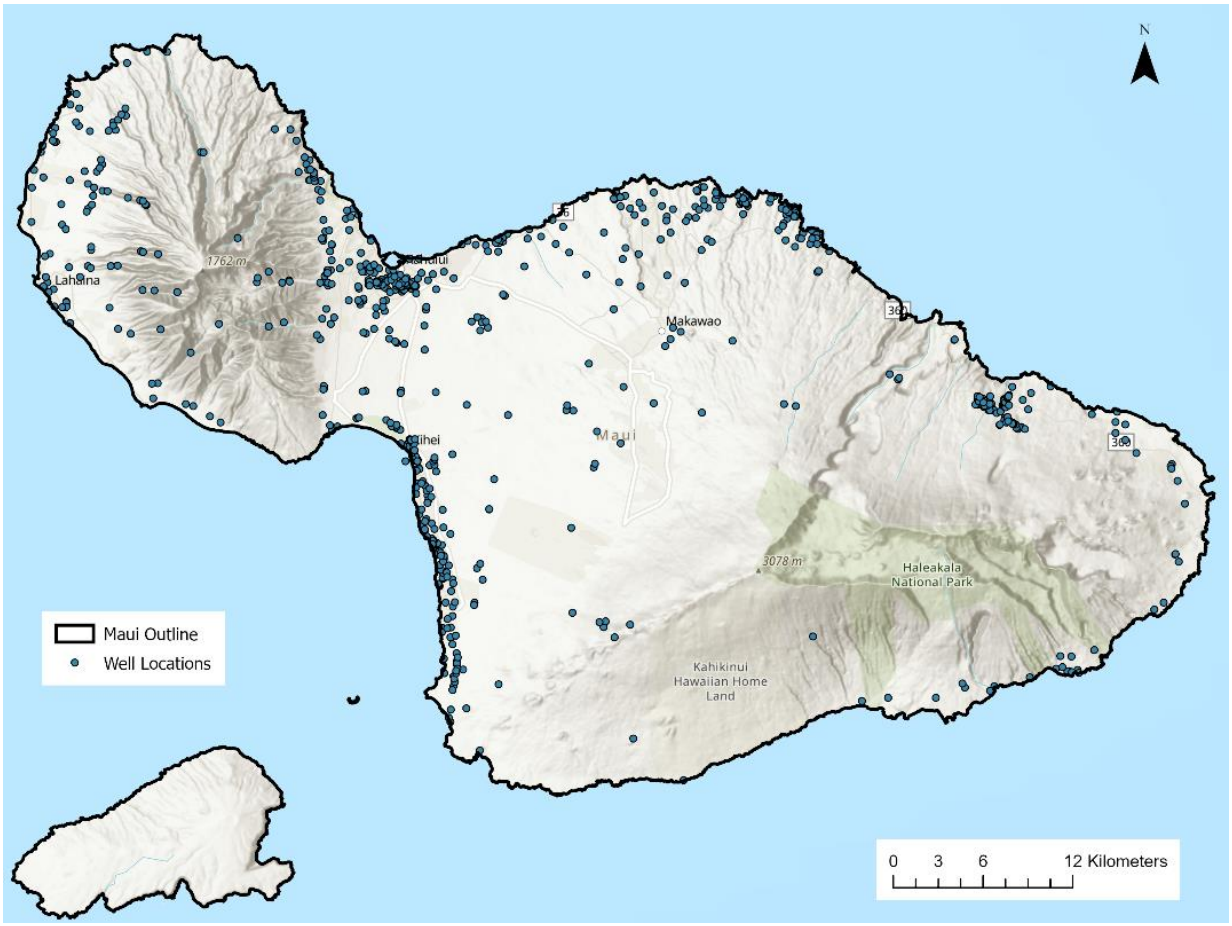

Figure A1. Well locations in Maui, Hawaii that were used to create the well density map. Well locations were acquired from the Hawaii State Water Wells project through the Hawaii Groundwater & Geothermal Resources Center, with data spanning from 1987–2012.

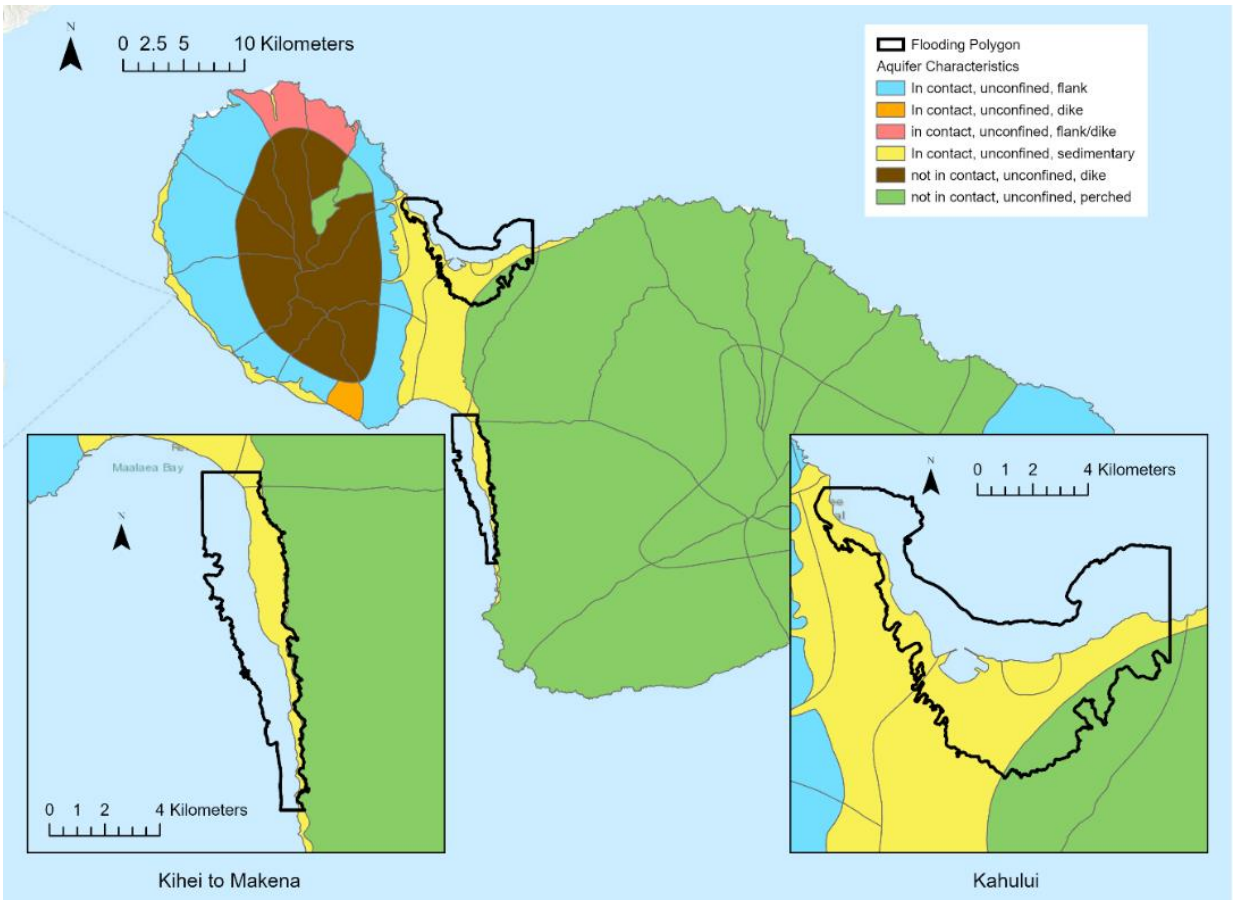

Figure A2. Aquifer types in Maui, Hawaii used for saltwater intrusion risk analysis and data tabulation. The Kihei–Makena study region is shown in the bottom left corner, and the Kahului study region is shown in the bottom right corner.

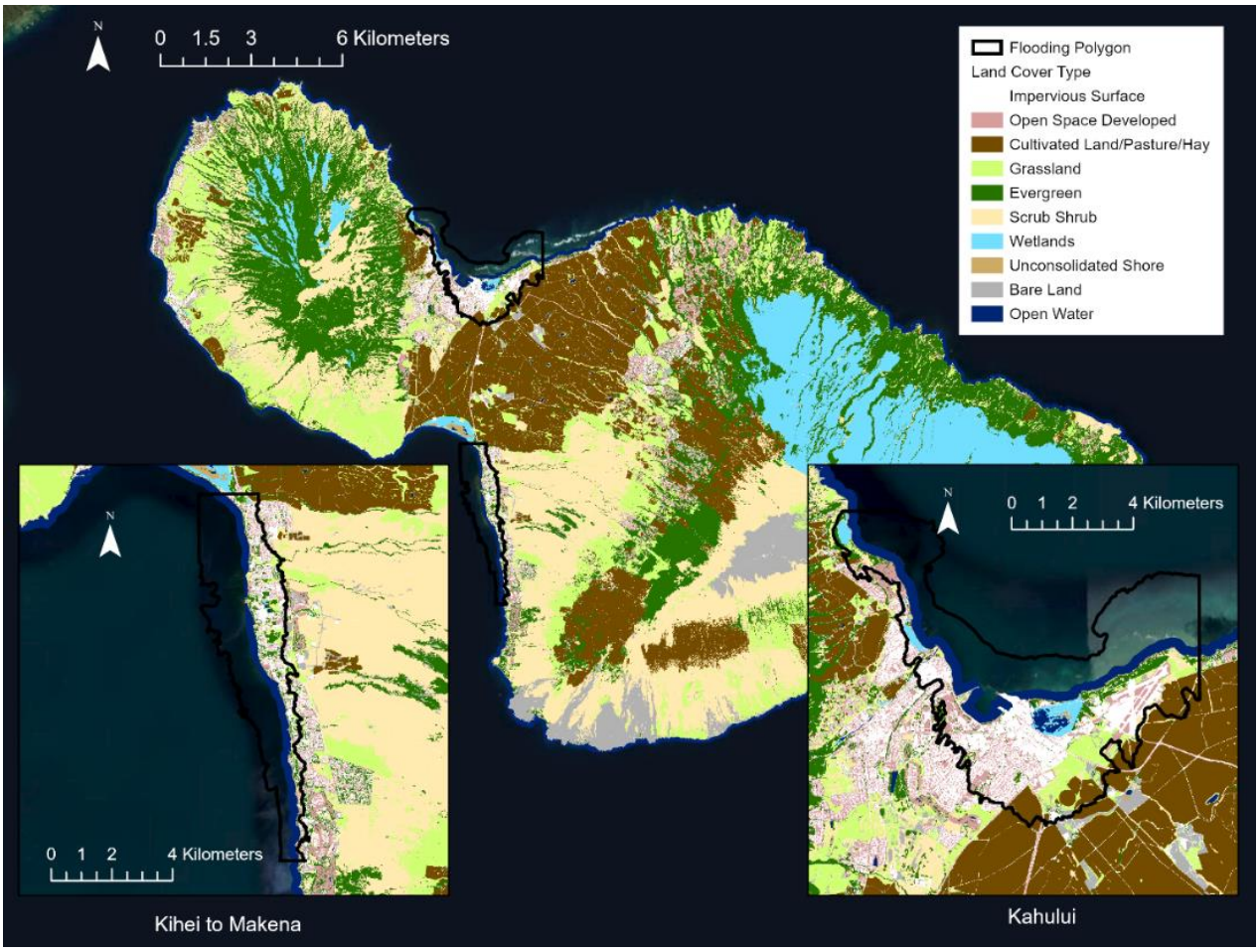

Figure A3. Overview of land cover classes present in Maui, Hawaii, with Kihei–Makena displayed on the lower-left, and Kahului on the lower-right. Land cover classes were derived from the 2011 National Land Cover Dataset (NLCD).

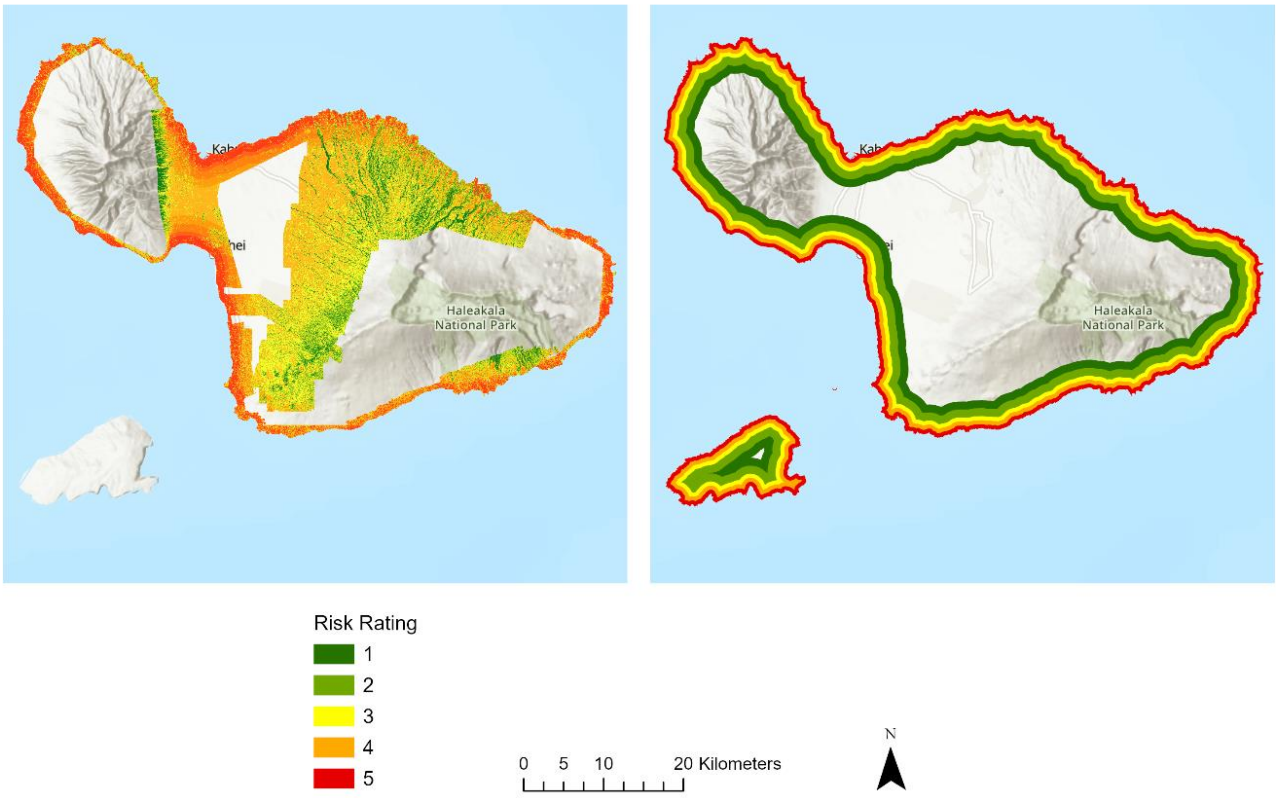

Figure A4. The slopes (left) across Maui and the distance (right) from shore thresholds were assigned a risk value of 1-5.

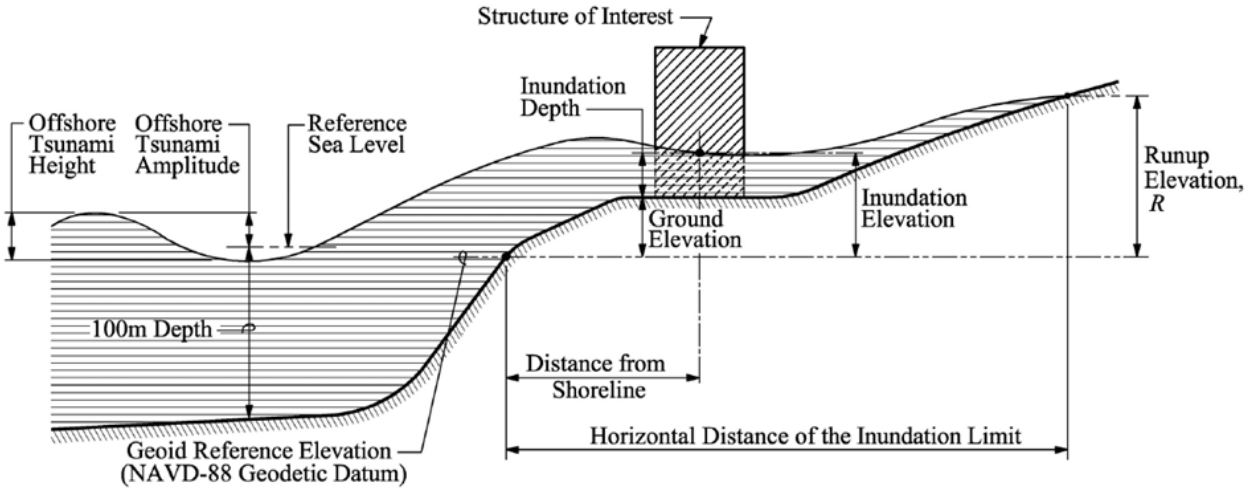

Figure A5. Key definitions in the ASCE tsunami design zone from the ASCE 7-16 Minimum Design Loads and Associated Criteria for Buildings and Other Structures.